Article

Cell Reports

Spinal Neuropeptide Y1 Receptor-Expressing Neurons Form an Essential Excitatory Pathway for Mechanical Itch

Graphical Abstract

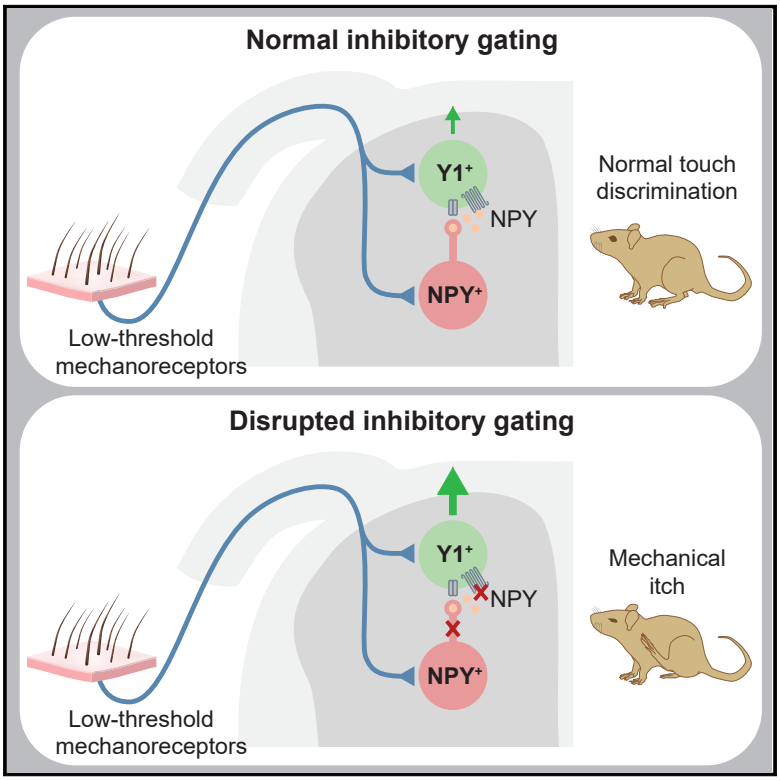

Highlights

- Excitatory NPYR1^{Cre} (Y1^{Cre}) neurons are required for mechanical itch transmission
- Spinal Y1^{Cre} neurons receive LTMR input and mediate light punctate touch
- NPY::Cre interneurons inhibit Y1-expressing neurons in the dorsal horn
- NPY signaling via dorsal horn Y1-expressing neurons gates mechanical itch

Authors

David Acton, Xiangyu Ren, Stefania Di Costanzo, ..., Ilaria Bertocchi, Carola Eva, Martyn Goulding

Correspondence

goulding@salk.edu

In Brief

Acton et al. identify the excitatory neurons in the dorsal spinal cord that drive mechanical itch. These cells mediate responses to light punctate touch and are inhibited by neuropeptide Y (NPY)::Cre interneurons. Light touch sensitivity and mechanical itch responses are gated by NPY signaling mediated by Y1-expressing neurons in the dorsal horn.

Acton et al., 2019, Cell Reports *28*, 625–639
July 16, 2019
https://doi.org/10.1016/j.celrep.2019.06.033

CellPress

Cell Reports
Article

Spinal Neuropeptide Y1 Receptor-Expressing Neurons Form an Essential Excitatory Pathway for Mechanical Itch

David Acton,[1] Xiangyu Ren,[1,2] Stefania Di Costanzo,[1,2] Antoine Dalet,[1] Steeve Bourane,[1,4] Ilaria Bertocchi,[3] Carola Eva,[3] and Martyn Goulding[1,5,*]
[1]Molecular Neurobiology Laboratory, The Salk Institute for Biological Studies, 10010 North Torrey Pines Road, La Jolla, CA 92037, USA
[2]Biology Graduate Program, Division of Biological Sciences, University of California, San Diego, 9500 Gilman Drive, La Jolla, CA 92093, USA
[3]Department of Neuroscience, University of Torino, Neuroscience Institute of the Cavalieri-Ottolenghi Foundation, Regione Gonzole 1, 10043 Orbassano, Italy
[4]Present address: Université de la Réunion, Dé Troi, UMR 1188 INSERM, 2 Rue Maxime Rivière, 97490 Sainte Clotilde, France
[5]Lead Contact
*Correspondence: goulding@salk.edu
https://doi.org/10.1016/j.celrep.2019.06.033

SUMMARY

Acute itch can be generated by either chemical or mechanical stimuli, which activate separate pathways in the periphery and spinal cord. While substantial progress has been made in mapping the transmission pathway for chemical itch, the central pathway for mechanical itch remains obscure. Using complementary genetic and pharmacological manipulations, we show that excitatory neurons marked by the expression of the neuropeptide Y1 receptor ($Y1^{Cre}$ neurons) form an essential pathway in the dorsal spinal cord for the transmission of mechanical but not chemical itch. Ablating or silencing the $Y1^{Cre}$ neurons abrogates mechanical itch, while chemogenetic activation induces scratching. Moreover, using *Y1* conditional knockout mice, we demonstrate that endogenous neuropeptide Y (NPY) acts via dorsal-horn Y1-expressing neurons to suppress light punctate touch and mechanical itch stimuli. NPY-Y1 signaling thus regulates the transmission of innocuous tactile information by establishing biologically relevant thresholds for touch discrimination and mechanical itch reflexes.

INTRODUCTION

Itch is a protective cutaneous somatosensory modality that drives reflexive scratching to remove harmful parasites and irritants from the skin. Itch is elicited either by chemical pruritogens, including histamine and serotonin, or by light mechanical stimuli, such as an insect crawling across the skin (Dong and Dong, 2018; Hachisuka et al., 2018; Han and Dong, 2014; Ikoma, 2013; Ikoma et al., 2006). Although chemical and mechanical itch function in a complementary manner to protect against cutaneous tissue damage, there is growing evidence that they are mediated by separate neural pathways in the periphery and spinal cord.

The transmission pathway for chemical itch has been characterized in some detail (Bautista et al., 2014; Dong and Dong, 2018; Hachisuka et al., 2018; Ikoma, 2013). Chemical pruritogens activate pruriceptive Aδ and C fibers that display little or no mechanical sensitivity (Ringkamp et al., 2011; Schmelz et al., 1997, 2003), and these convey the itch signal from the skin to the superficial dorsal horn. Within the dorsal horn, chemical itch is transmitted by neurons expressing the gastrin releasing peptide receptor (GRPR) (Bautista et al., 2014; Hachisuka et al., 2018; Han and Dong, 2014; Mishra and Hoon, 2013; Sun et al., 2009; Sun and Chen, 2007). Thereafter, the signal is relayed to the thalamus (Davidson et al., 2007, 2012; Johanek et al., 2008; Ma et al., 2012; Papoiu et al., 2012; Simone et al., 2004) and parabrachial nucleus (Campos et al., 2018; Mu et al., 2017) by projection neurons, including those marked by neurokinin-1 receptor (NK1R) expression (Akiyama et al., 2015). Much less is known about mechanical itch, which is initiated by the activation of low-threshold mechanoreceptors (LTMRs) in the skin (Fukuoka et al., 2013; Han and Dong, 2014; Koch et al., 2018). Recently, we showed that mechanical itch is selectively gated by inhibitory interneurons in the dorsal horn that are marked by the expression of *Neuropeptide Y::Cre* (NPY::Cre interneurons [INs]). Ablation of NPY::Cre INs in mice leads to chronic scratching in the absence of an external stimulus, as well as an increased tendency to scratch in response to low-threshold mechanical stimulation of the nape, consistent with disinhibited transmission of tactile information from the hairy skin (Bourane et al., 2015a). This mechanical itch phenotype is independent of the $GRPR^{+}$ neuron-dependent chemical itch pathway, providing strong evidence for a separate mechanical itch pathway in the spinal cord. However, the excitatory spinal neurons that transmit the mechanical itch signal and the mechanism by which the inhibitory NPY::Cre INs gate the flow of information through this pathway remain wholly unknown.

In this study, we delineate a central circuit for the processing of mechanical itch that incorporates a peptidergic signaling

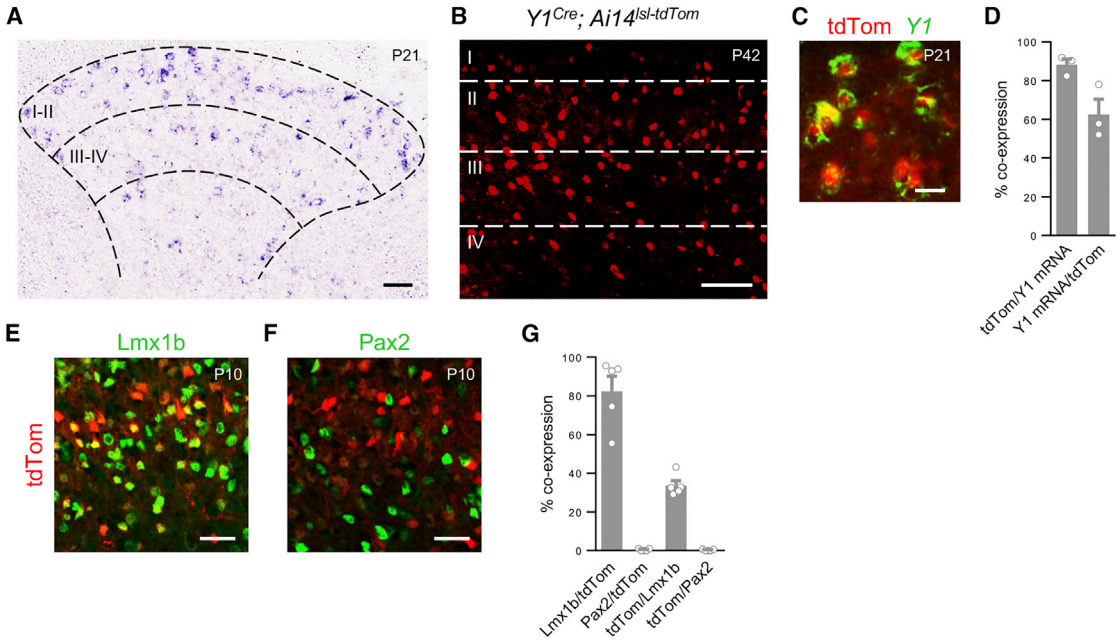

Figure 1. $Y1^{Cre}$ Marks a Population of Excitatory Neurons Concentrated in Laminae II-III

(A) Transverse section through the lumbar spinal cord of a P21 mouse showing *Y1* mRNA expression in the dorsal horn.

(B) Section from a P42 $Y1^{Cre}$; $Ai14^{lsl\text{-}tdTom}$ mouse showing laminar distribution of Y1-tdTomato neurons.

(C) Co-expression of tdTomato and *Y1* mRNA in the dorsal horn of a P21 $Y1^{Cre}$; $Ai14^{lsl\text{-}tdTom}$ mouse.

(D) Summary of *Y1* mRNA expression (n = 3 mice).

(E and F) Transverse sections through the lumbar spinal cord of a P10 $Y1^{Cre}$; $Ai14^{lsl\text{-}tdTom}$ mouse stained with antibodies against Lmx1b (E) and Pax2 (F).

(G) Quantification of co-expression of Y1-tdTomato with antibody-labeled Lmx1b and Pax2 in P10 $Y1^{Cre}$; $Ai14^{lsl\text{-}tdTom}$ mice (n = 5 mice). Roman numerals denote Rexed's laminae.

Scale bars: 50 μm (A, B, E, and F) and 10 μm (C). Data: mean ± SEM. See also Figures S1–S3.

mechanism to establish normal touch discrimination. We show that neurons in the dorsal spinal cord expressing Y1 and the transcription factor Lbx1, hereafter referred to as $Y1^{Cre}$ neurons, are essential for the central transmission of light punctate touch and mechanical but not chemical itch. Ablating the spinal $Y1^{Cre}$ neurons abolishes the chronic spontaneous scratching that occurs following removal of the NPY::Cre INs, while ablation or silencing spinal $Y1^{Cre}$ neurons renders mice insensitive to mechanical but not chemical stimulation. We go on to demonstrate that endogenous NPY acts on $Y1^{+}$ dorsal horn neurons to suppress light punctate touch and mechanical itch. $Lbx1^{Cre}$; $Y1^{f/f}$ conditional knockout mice exhibit spontaneous scratching and hypersensitivity to mechanical itch stimuli, as well as reduced thresholds for hindpaw withdrawal from light punctate stimuli, but, like $Y1^{Cre}$ neuron-ablated mice, they have normal responses to chemical itch and pain stimuli. Conversely, selective activation of Y1 receptors or activation of NPY::Cre INs to stimulate endogenous NPY release reduces mechanical itch responses. These data show that the mechanical itch pathway is gated by NPY-Y1 signaling within the dorsal horn. These data also indicate that the previously reported analgesic effects of NPY and Y1 signaling (Diaz-delCastillo et al., 2018; Duggan et al., 1991; Hua et al., 1991; Intondi et al., 2008; Naveilhan et al., 2001; Solway et al., 2011; Taiwo and Taylor, 2002) are mediated by peripheral sensory neurons.

RESULTS

Y1 Expression Marks a Population of Excitatory Neurons within the LTMR-RZ

Mechanical itch is mediated by light touch information transmitted to the spinal cord by LTMRs innervating the hairy skin (Fukuoka et al., 2013); this information is then subject to inhibitory gating by locally projecting NPY::Cre INs in the dorsal horn (Bourane et al., 2015a). We therefore centered our search for the excitatory neurons that transmit the mechanical itch signal on glutamatergic cells that are located within the LTMR recipient zone (LTMR-RZ) of the dorsal horn (Abraira et al., 2017). This zone (laminae IIi–IV) contains molecularly diverse excitatory populations that are extensively innervated by LTMRs (Abraira et al., 2017; Abraira and Ginty, 2013; Koch et al., 2018). Of particular interest was a subset of dorsal horn excitatory neurons distinguished by expression of the inhibitory Y1 receptor (NPYR1; Häring et al., 2018; Melnick, 2012; Miyakawa et al., 2005; Sathyamurthy et al., 2018). *Y1* mRNA-positive neurons are distributed throughout the LMTR-RZ and are also present in laminae I–IIo (Figure 1A). In the spinal cords of adult $Y1^{Cre}$ ($NPYR1^{Cre}$) knockin mice (Padilla et al., 2016) carrying the $Ai14^{lsl\text{-}tdTom}$ reporter (Madisen et al., 2010), $Y1^{Cre}$-derived cells were enriched in laminae IIi/III, with additional cells present in laminae I, IIo, and IV (Figures 1B and S1C). 88.8% ± 2.0% of

Y1^{+} cells in the dorsal horn co-expressed the *Y1*^{Cre}-dependent tdTomato reporter, with 62.5% ± 7.9% of tdTomato^{+} neurons showing *Y1* expression (Figures 1C and 1D). Likewise, when *Y1*^{Cre}; *Ai14*$^{lsl\text{-}tdTom}$ mice were crossed with a *Y1::EGFP* transgenic reporter line (Gene Expression Nervous System Atlas [GENSAT]), 84.4% ± 4.6% of the EGFP^{+} neurons co-expressed tdTomato (Figures S1A–S1C) and 53.8% ± 3.4% of the tdTomato^{+} neurons co-expressed EGFP. These data suggest that *Y1*^{Cre} captures dorsal horn neurons that exhibit transient or low-level *Y1* gene expression in addition to cells that show persistent expression, as has been noted for other Cre drivers (e.g., Bourane et al., 2015a; Duan et al., 2014; Peirs et al., 2015).

The vast majority of *Y1*^{Cre}-derived neurons are excitatory, with 82.4% ± 6.9% expressing Lmx1b and only 0.4% ± 0.2% expressing the inhibitory neuron marker Pax2 (Figures 1E–1G). Furthermore, some tdTomato^{+} cells co-expressed markers of excitatory neuron populations that have been implicated in the transmission of mechanical stimuli, including cMaf^{+} neurons (Wende et al., 2012), retinoid-related orphan receptor alpha (RORα)$^{+}$ neurons (Bourane et al., 2015b), and Somatostatin (Sst)$^{+}$ neurons (Christensen et al., 2016; Duan et al., 2014; Huang et al., 2018). Co-expression was also seen in gastrin releasing peptide (GRP)-expressing neurons (Mishra and Hoon, 2013; Solorzano et al., 2015), as well as in NK1R^{+} neurons in lamina I and laminae III–IV (Akiyama et al., 2013, 2015; Carstens et al., 2010). By contrast, there was no overlap with neurons that express GRPR, or cells expressing the astrocytic markers S100β or glial fibrillary acidic protein (GFAP) (Figure S2).

In keeping with this analysis, sparse labeling of Y1^{Cre} neurons in laminae I–IV with EnvA-pseudotyped ΔG-dsRed-Express rabies virus revealed cell morphologies that are characteristic of excitatory neurons. These include central-, vertical-, and radial-like cell types in lamina II (Grudt and Perl, 2002), and projection neurons in lamina I that likely correspond to NK1R^{+} projection neurons (Akiyama et al., 2015; Brumovsky et al., 2006; Szabo et al., 2015). We also observed fusiform neurons in lamina II and multipolar neurons in laminae III–IV, some of which were previously shown to express Y1 (Figure S3; Brumovsky et al., 2006).

To determine whether Y1^{Cre} neurons receive direct LTMR inputs, we performed injections of cholera toxin B (CTb) into either the hairy skin of the thigh or the glabrous skin of the plantar hindpaw of adult *Y1*^{Cre}; *Ai14*$^{lsl\text{-}tdTom}$ mice. CTb-labeled boutons from fibers innervating either region were found in close apposition to Y1^{Cre}-tdTomato somata, and many of these displayed immunoreactivity for vesicular glutamate transporter 1 (vGluT1), which labels myelinated Aß and Aδ LTMRs in the LTMR-RZ (Figures 2A and 2B; n = 3 mice assessed per condition) (Todd et al., 2003).

The LTMR subtypes that innervate Y1^{Cre} neurons were further analyzed by intersectional monosynaptic retrograde tracing with EnvA-pseudotyped ΔG-mCherry rabies virus (Figures 2C–2J) (Albisetti et al., 2017; Bourane et al., 2015a, 2015b; Wickersham et al., 2007). Retrograde mCherry expression was observed in multiple cutaneous LTMR subtypes, including c-Ret^{+}/IB4^{-} Aß-LTMRs, TrkC^{+}/parvalbumin^{-} Aß-LTMRs, TrkB^{+} Aδ-LTMRs, and putative LTMRs that express calcitonin gene-related peptide (CGRP) and neurofilament 200 (NF200) (Bourane et al., 2015b; Lawson et al., 2002). Dorsal root ganglion (DRG) neurons expressing calbindin, which innervate Meissner corpuscles, were also labeled (Figure 2I). Proprioceptors marked by the expression of parvalbumin were largely spared, and Aß fibers expressing calretinin, which innervate Pacinian corpuscles, were never detected (Figure 2J). In summary, this analysis provides clear evidence that the Y1^{Cre} neurons are extensively innervated by cutaneous LTMR fibers.

Y1^{Cre} Neurons Are Essential Components of the Mechanical Itch Pathway Gated by Inhibitory NPY::Cre INs

NPY::Cre IN ablation causes a mechanical itch phenotype that is marked by increased spontaneous hindlimb scratching (Figure 3A; Bourane et al., 2015a). We therefore set about examining whether the Y1^{Cre} neurons in the dorsal horn transmit the mechanical itch signal using a genetic epistasis strategy entailing diphtheria toxin (DT)-mediated ablation of both the *NPY::Cre/Lbx1* and *Y1*^{Cre}*/Lbx1* populations. Ablation of dorsal horn NPY::Cre INs alone significantly increased spontaneous scratching 1 week after DT treatment, from 12 ± 2 scratch episodes per 30-min observation period in FlpO^{-} controls to 100 ± 17 episodes in ablated animals (Figures 3A, S4A, S4D, and S4E). Strikingly, this increase in spontaneous scratching was completely abolished following ablation of both the Y1^{Cre} and NPY::Cre populations in DT-treated *Y1*^{Cre}; *NPY::Cre*; *Lbx1*^{FlpO}; *Tau*$^{ds\text{-}DTR}$; *Ai65*$^{ds\text{-}tdTom}$ mice (Figures 3A, S4B, S4D, and S4E). These findings demonstrate that the Y1^{Cre} neurons are required for the expression of the mechanical itch phenotype in mice lacking *NPY::Cre*-derived inhibitory INs.

Sst expression partially overlaps with Y1 expression in lamina II (Figures S2E–S2G; Zhang et al., 1999), and Sst signaling has been implicated in chemical itch transmission (Christensen et al., 2016; Huang et al., 2018; Kardon et al., 2014). We therefore set out to test whether NPY::Cre IN-gated scratching is mediated by Sst^{+} neurons in the dorsal horn. Strikingly, in contrast to the negation of scratching that occurs upon Y1^{Cre} neuron depletion in NPY::Cre IN-ablated mice, simultaneous ablation of the NPY::Cre and Sst^{+} populations did not reduce scratching as compared to NPY::Cre IN-ablated controls (Figures 3A and S4C–S4E; $p > 0.05$). Furthermore, removing the Sst^{+} neurons alone did not alter spontaneous scratching or responses to mechanical stimulation of the nape (Figure S5). These data reveal that dorsal horn neurons expressing Y1, either transiently or persistently, are necessary for transmitting the light touch modalities that drive mechanical itch, whereas those that express Sst, including Sst^{+}/Y1^{+} neurons, are not.

Y1^{Cre} Neurons Selectively Transmit the Mechanosensory Stimuli That Drive Mechanical Itch

We next examined the function of the Y1^{Cre} neurons in transmitting the itch sensation that is generated by low-threshold mechanical irritation of the hairy skin. Mechanical itch induction was assessed using a modified alloknesis assay (Akiyama et al., 2012) in which a low-force (0.16 g) von Frey hair was applied to the hairy skin of the nape, and scratching responses were recorded over ten trials. Whereas nape stimulation elicited scratching in 22.7% ± 4.7% of trials in control mice, it did so in only 3.6% ± 2.3% of trials in which the Y1^{Cre} neurons were ablated

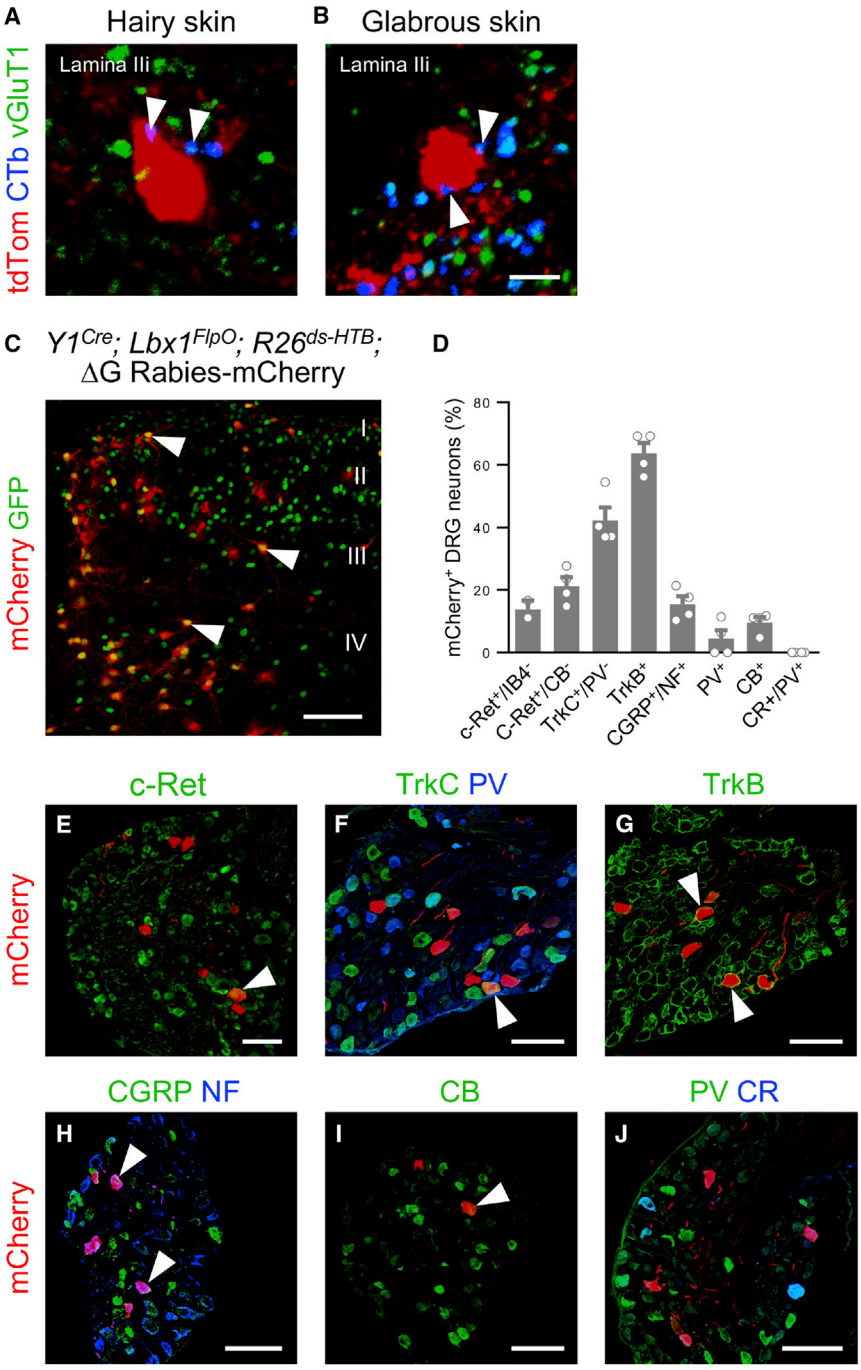

Figure 2. *Y1*^{Cre} Neurons Receive Extensive LTMR Input

(A and B) Examples of Y1^{Cre} neurons in lamina IIi from lumbar spinal cord sections of P42 *Y1*^{Cre}; *Ai14*$^{lsl\text{-}tdTom}$ mice injected with CTb into: the hairy skin of the thigh (A) and the glabrous skin of the hindpaw (B). Immunolabeled CTb^{+} contacts (blue) displayed vGluT1 immunoreactivity (green, arrowheads).

(C) Section through the lumbar dorsal horn of a P10 *Y1*^{Cre}; *Lbx1*^{FlpO}; *R26*$^{ds\text{-}HTB}$ mouse injected with EnvA G-deleted rabies-mCherry virus. Arrowheads indicate infected Y1^{Cre} neurons. mCherry^{+}/GFP^{-} cells represent transsynaptically labeled presynaptic neurons.

(D) Summary of antibody-labeled myelinated sensory afferent subtypes that are presynaptic to the Y1^{Cre} neurons, expressed as a percentage of mCherry^{+} neurons (n = 4 mice).

(E–J) Sections from P10 *Y1*^{Cre}; *Lbx1*^{FlpO}; *R26*$^{ds\text{-}HTB}$ lumbar DRGs showing presynaptically labeled sensory neurons(red) that express c-Ret (E), TrkC but not parvalbumin (PV; F), TrkB (G), calcitonin gene-related peptide (CGRP) and neurofilament 200 (NF; H), and calbindin (CB; I), but not PV or calretinin (CR; J). Arrowheads indicate co-labeled sensory afferents. CB, calbindin; CR, calretinin; NF, neurofilament; PV, parvalbumin. Scale bars: 5 μm (B) and 100 μm (C and E–J). Data: mean ± SEM. See also Figure S4.

(Figures 3B and S6A–S6B). A similar reduction in scratching was observed when the Y1^{Cre} neurons were silenced in *Y1*^{Cre}; *Lbx1*^{FlpO}; *R26*$^{ds\text{-}hM4D}$ mice treated with clozapine *N*-oxide (CNO), as compared with CNO-treated *Y1*^{Cre}; *R26*$^{ds\text{-}hM4D}$ control mice that lack FlpO-dependent expression of the hM4D receptor (Figure 3C). Conversely, scratching was greatly enhanced when the Y1^{Cre} neurons were activated in *Y1*^{Cre}; *Lbx1*^{FlpO}; *R26*$^{ds\text{-}hM3D}$ animals (Figure 3D), which is consistent with heightened sensitivity to low-threshold tactile stimulation. There was also a marked increase in the number of spontaneous hindlimb scratching bouts over a 30-min period following hM3D-mediated activation of the Y1^{Cre} neurons (Figure 3E).

We then considered the possibility that the increases in spontaneous and evoked scratching seen in *Y1*^{Cre}; *Lbx1*^{FlpO}; *R26*$^{ds\text{-}hM3D}$ mice might be attributable to the activation of the chemical itch pathway that is dependent on GRPR^{+} neurons. As previously shown, chloroquine-induced chemical itch was strongly reduced in wild-type mice following ablation of the GRPR^{+} neurons by intrathecal (i.t.) injection of saporin-conjugated bombesin (BOM-SAP; Figures S6C–S6E) (Bourane et al., 2015a; Huang et al., 2018; Sun et al., 2009). By contrast, scratching responses to nape stimulation were unaffected (Figure 3F). Consistent with these results, neither the evoked nor spontaneous scratching seen following activation of Y1^{Cre} neurons was affected by ablation of the GRPR^{+} neurons (Figures 3G and 3H). These data agree with our previous report that spontaneous scratching induced by removal of NPY::Cre INs is not affected by ablation of the GRPR^{+} neurons (Bourane et al., 2015a), despite our finding that the Y1^{Cre} neurons include some GRP-expressing neurons (Figures S2C, S2F, and S2G).

We next considered whether the pathways for chemical and mechanical itch transmission converge downstream of the GRPR^{+} neurons on lamina I NK1R^{+} neurons, given that *Y1*^{Cre}

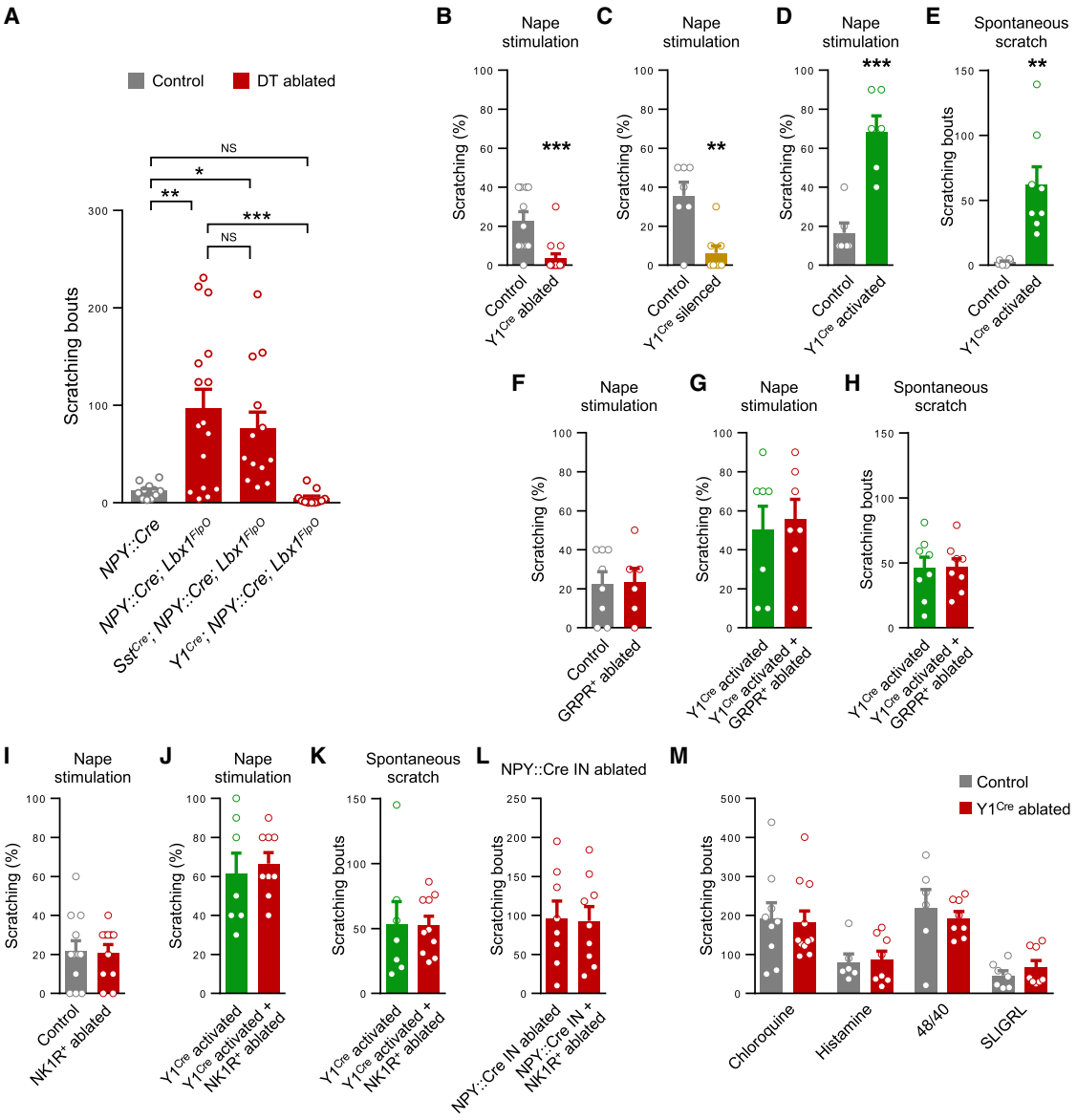

Figure 3. Y1^{Cre} Neurons within the Dorsal Horn Transmit Mechanical but Not Chemical Itch

(A) Ablation of dorsal horn NPY::Cre INs increases spontaneous scratching in *NPY::Cre; Lbx1^{FlpO}; Tau$^{ds\text{-}DTR}$; Ai65$^{ds\text{-}tdTom}$* mice (n = 16) compared with DT-treated *NPY::Cre; Tau$^{ds\text{-}DTR}$; Ai65$^{ds\text{-}tdTom}$* controls that lack DT-receptor expression (n = 11). Ablation of the Y1^{Cre} and NPY::Cre IN populations in *Y1^{Cre}; NPY::Cre; Lbx1^{FlpO}; Tau$^{ds\text{-}DTR}$; Ai65$^{ds\text{-}tdTom}$* mice abolishes scratching (n = 11). Scratching is unaffected when Sst^{+} neurons are ablated together with the NPY::Cre INs in *Sst^{Cre}; NPY::Cre; Lbx1^{FlpO}; Tau$^{ds\text{-}DTR}$; Ai65$^{ds\text{-}tdTom}$* mice (n = 13). One-way ANOVA and Bonferroni post hoc tests were used to assess statistical differences.

(B and C) Reduced scratching in response to stimulation of the nape with a 0.16-g von Frey hair in *Y1^{Cre}; Lbx1^{FlpO}; Tau$^{ds\text{-}DTR}$; Ai65$^{ds\text{-}tdTom}$* mice treated with DT (n = 14) compared with saline-treated controls (n = 11; B), and in *Y1^{Cre}; Lbx1^{FlpO}; R26$^{ds\text{-}hM4D}$* mice treated with clozapine *N*-oxide (CNO; n = 8) compared with *Y1^{Cre}; R26$^{ds\text{-}hM4D}$* controls, which lack FlpO-dependent hM4D expression (n = 8; C).

(D) Enhanced scratching in response to stimulation of the nape in CNO-treated *Y1^{Cre}; Lbx1^{FlpO}; R26$^{ds\text{-}hM3D}$* mice (n = 6) compared with *Y1^{Cre}; R26$^{ds\text{-}hM3D}$* controls (n = 6).

(E) Spontaneous scratching in CNO-treated *Y1^{Cre}; Lbx1^{FlpO}; R26$^{ds\text{-}hM3D}$* mice (n = 8) is enhanced over a 30-min period compared with control mice (n = 6).

(F) Scratching responses are unchanged in wild-type mice treated with bombesin-saporin (BOM-SAP; n = 6) to ablate GRPR^{+} neurons compared with controls injected with saporin (SAP; n = 8).

(G and H) Ablation of GRPR^{+} neurons in *Y1^{Cre}; Lbx1^{FlpO}; R26$^{ds\text{-}hM3D}$* mice does not alter evoked scratching (G; BOM-SAP, n = 8; SAP, n = 7) or spontaneous scratching (H; BOM-SAP, n = 7; SAP, n = 7) following CNO injection.

(I) Scratching responses are unchanged in wild-type mice treated with [Sar^{9}, Met(O$_2$)^{11}]-substance P-SAP (SSP-SAP; n = 10) to ablate NK1R^{+} neurons compared to SAP-injected controls (n = 11).

(legend continued on next page)

and NK1R expression partially overlap (Figures S2D, S2F, and S2G) and evidence that NK1R$^+$ projection neurons convey chemical itch sensation to key supraspinal regions for the integration of aversive stimuli (Carstens et al., 2010; Akiyama et al., 2013, 2015). Ablation of the NK1R$^+$ neurons by injection of saporin conjugated to the NK1R ligand [Sar^9, Met(O$_2$)^{11}]-substance P (SSP-SAP) significantly attenuated chloroquine-induced itch (Figures S6F–S6H) consistent with previous reports (Carstens et al., 2010). However, NK1R$^+$ neuron ablation failed to modulate mechanically evoked itch in wild-type mice (Figure 3I), nor did it alter the rate of evoked or spontaneous scratching that occurs when the Y1^{Cre} neurons are activated (Figures 3J and 3K). Ablation of the NK1R$^+$ neurons also did not alleviate scratching induced by ablation of NPY::Cre INs (Figure 3L).

As a final test to exclude the possibility that Y1^{Cre} neurons are interposed in the chemical itch circuitry, we assessed scratching in Y1^{Cre} neuron-ablated mice following injection of chloroquine, histamine, compound 48/80 or SLIGRL into the skin behind the ear. Scratching responses to all four pruritogens remained intact in Y1^{Cre} neuron-ablated mice (Figure 3M), confirming that these cells are not required for chemical itch, Together, these data indicate that that the minority of Y1^{Cre} neurons that co-express NK1R are dispensable for mechanical itch sensation.

Our demonstration that the Y1^{Cre} neurons are essential for mechanical itch led us to ask whether the Y1^{Cre} neurons have a role in transmitting low-threshold mechanical stimuli. Sensitivity to light punctate touch, as assessed by von Frey hair stimulation of the glabrous skin, was significantly reduced after ablating or silencing the Y1^{Cre} neurons (Figures 4A and 4B). Conversely, sensitivity was elevated by activation of the Y1^{Cre} neurons (Figure 4C). However, responses to light dynamic touch, as assessed by gentle brushing, were unaffected (Figure 4D). This finding is consistent with our observation that there is little, if any, overlap between the Y1^{Cre} and RORα^+ neuronal populations (Figures S2B, S2F, and S2G), the latter of which transmits dynamic touch (Bourane et al., 2015b). Sensitivity to acute pain, as assessed by the pinprick and Randall-Sellito tests, was largely unchanged in Y1^{Cre} neuron-ablated mice, as were responses to pain chemically induced by intradermal injection of capsaicin or formalin. Thermal pain, as assessed by the hot-plate and Hargreaves assays, was likewise unaffected (Figures 4E–4J). Together, these findings suggest that the Y1^{Cre} population of neurons is largely specialized for transmitting light touch information, and they play little or no role in relaying chemical itch, noxious mechanical, or thermal information.

NPY Peptide Signaling Regulates Mechanical Itch Transmission

The underlying signaling mechanisms that contribute to the gating of mechanical itch by the NPY::Cre INs have not been established. In *Y1::EGFP*; *NPY::Cre* mice injected intraspinally (T_{13}-L_1 levels) with an AAV2/1-hSyn-DIO-SypHTomato virus, lamina II EGFP$^+$ cell bodies displayed tdTomato$^+$ synaptic contacts from NPY::Cre INs (Figures 5A and 5B; n = 3 mice). These contacts colocalized with vesicular GABA (gamma-aminobutyric acid) transporter (VGAT), indicating that NPY::Cre INs provide inhibitory synaptic inputs to Y1$^+$ neurons (Figure 5A). Strikingly, many puncta also had NPY immunoreactivity (Figure 5B), with multiple NPY immunoreactive puncta being co-localized with the postsynaptic marker gephyrin on Y1-tdTomato$^+$ somata in *Y1^{Cre}*; *Ai14$^{lsl\text{-}tdTom}$* mice (Figure 5C; n = 3).

To confirm that the NPY::Cre INs form functional synapses onto Y1$^+$ neurons, we performed whole-cell patch-clamp recordings from lamina IIi Y1-EGFP cells in spinal cord sections from *Y1::EGFP*; *NPY::Cre*; *Lbx1^{FlpO}*; *R26$^{ds\text{-}ReaChR}$* mice (Hooks et al., 2015). Following current injection, the Y1-EGFP neurons displayed either single (20%) or phasic firing patterns (80%; n = 32) that are characteristic of dorsal excitatory neurons (Abraira et al., 2017; Grudt and Perl 2002; Koch et al., 2018). We then blocked glutamatergic transmission with kynurenic acid and recorded from Y1-EGFP neurons at a holding potential of −30 mV. Under these conditions, we observed inhibitory currents in 11/30 neurons following red-light excitable channelrhodopsin (ReaChR)-mediated activation of the NPY::Cre INs (mean amplitude: 57.3 ± 15.6 pA). These currents were abolished in 7/7 neurons following application of strychnine and picrotoxin (Figures 5D–5F), demonstrating the NPY::Cre INs form functional inhibitory synapses onto excitatory Y1$^+$ neurons within the dorsal horn.

The intriguing finding that the Y1^{Cre} neurons are contacted by processes containing putative NPY$^+$ dense core vesicles suggested to us that NPY peptidergic signaling via the Y1^{Cre} neurons might also contribute to the gating of the mechanical itch pathway. To assess the role of G$_i$-mediated inhibitory Y1 signaling within the dorsal horn, we crossed *Lbx1^{Cre}* (Sieber et al., 2007) with *Y1$^{f/f}$* mice (Bertocchi et al., 2011) to remove *Y1* from dorsal horn neurons, sparing ventral, peripheral, and supraspinal neurons. *Lbx1^{Cre}*; *Y1$^{f/f}$* mice exhibited spontaneous scratching at P42, as well as elevated sensitivity to nape stimulation (Figures 6A and 6B). Similarly, both spontaneous and evoked scratching were elevated by the Y1 antagonist BIBP 3226 (Wang et al., 2016) acting at dorsal horn Y1 receptors (Figures 6C–6D and S7A–S7B). Likewise, elevated spontaneous scratching was observed following administration of another Y1 antagonist, BMS 193885 (Antal-Zimanyi et al., 2008), and in NPY knockout mice (Figure S7C) (Karl et al., 2008). Conditional knockout of *Y1* enhanced hindpaw sensitivity to light punctate touch but did not modulate responses to dynamic touch (Figures 6E and 6F) or the frequency of scratching in response to histaminergic and non-histaminergic chemical itch stimuli

(J and K) In *Y1^{Cre}*; *Lbx1^{FlpO}*; *R26$^{ds\text{-}hM3D}$* mice, ablation of NK1R$^+$ neurons does not alter evoked (J; SSP-SAP, n = 9; SAP, n = 7) or spontaneous (K; SSP-SAP, n = 10; SAP, n = 7) scratching following CNO injection.

(L) Unchanged scratching in *NPY::Cre; Lbx1^{FlpO}*; *Tau$^{ds\text{-}DTR}$*; *Ai65$^{ds\text{-}tdTom}$* mice 2 weeks after NK1R$^+$ neuron ablation and 1 week following DT administration (SSP-SAP, n = 9; SAP, n = 8).

(M) Unchanged scratching over a 30-min period in Y1^{Cre} neuron-ablated mice following injection of chloroquine (control, n = 9; ablated, n = 11), histamine (control, n = 6; ablated, n = 8), compound 48/80 (control, n = 6; ablated, n = 8), and SLIGRL (control, n = 7; ablated, n = 8).

*p < 0.05, **p < 0.01, ***p < 0.001, NS, not significant. Data: mean ± SEM. See also Figures S4–S6.

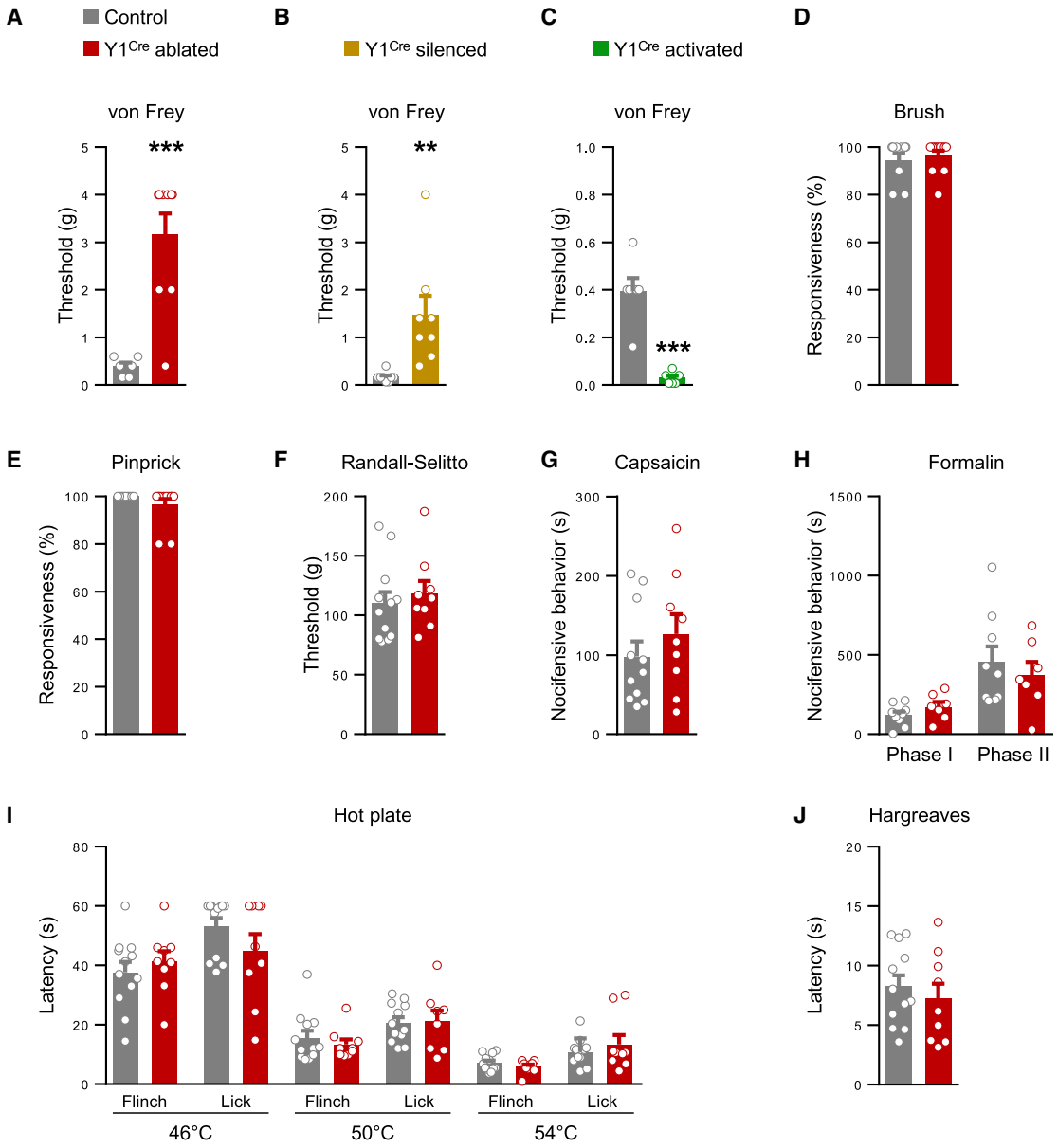

Figure 4. Y1^{Cre} Neurons Selectively Transmit Light Touch Information

(A and B) Sensitivity to von Frey hair stimulation of the hindpaw glabrous skin is reduced following Y1^{Cre} neuron ablation (A; control, n = 6; ablated, n = 9) or silencing (B; control, n = 8; silenced, n = 8).

(C) Glabrous skin sensitivity to von Frey hair stimulation is elevated following Y1^{Cre} neuron activation (control, n = 6; activated, n = 6).

(D–F) Responses to dynamic touch (D; control, n = 11; ablated, n = 13), pinprick (E; control, n = 11; ablated, n = 13), and Randall-Selitto (F; control, n = 12; ablated, n = 9) are unchanged after Y1^{Cre} neuron ablation.

(G and H) Chemical pain responses following hindpaw injection of capsaicin (G; control, n = 11; ablated, n = 9) or formalin (H; control, n = 9; ablated, n = 7) are not altered following Y1^{Cre} neuron ablation.

(I and J) Y1^{Cre} neuron-ablated mice show normal heat responses as assessed by the hot plate (I; control, n = 12; ablated, n = 9) and Hargreaves (J; control, n = 12; ablated, n = 9) assays.

**p < 0.01, ***p < 0.001. Data: mean ± SEM.

(Figure 6G). The duration and rate (duration/frequency) of scratching induced by compound 48/80 were also unchanged (Figures 6H and 6I; Gao et al., 2018). Likewise, responses to mechanical, chemical, and thermal pain stimuli were not affected (Figures 6J–6N). These data indicate that NPY-Y1 signaling in the dorsal horn has a selective role in the modulation of light punctate touch information from both the hairy and glabrous skin and, as a consequence, functions to gate mechanical itch.

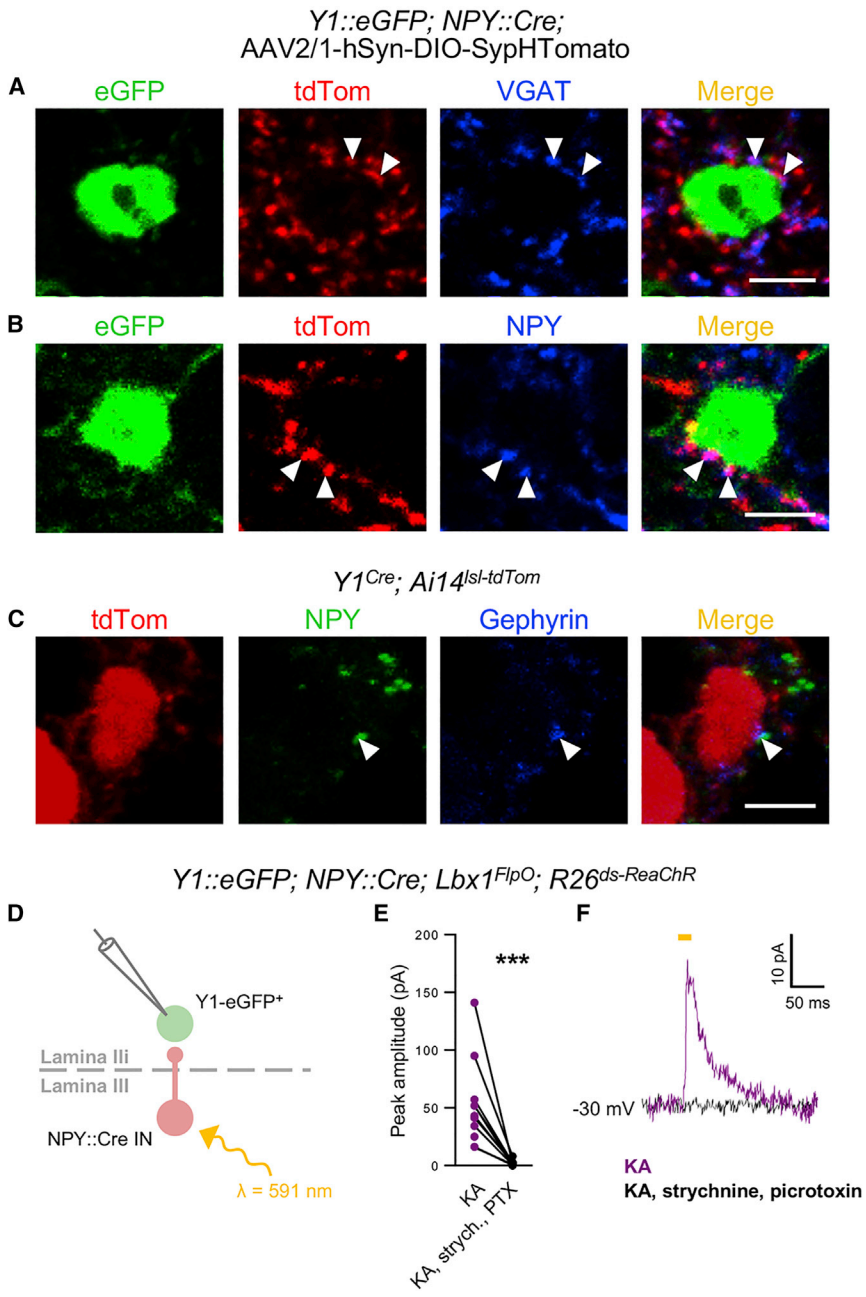

Figure 5. Y1^{Cre} Neurons Receive VGAT^{+} and NPY^{+} Synaptic Contacts from NPY::Cre INs

(A and B) Examples of GFP-labeled cells from the lumbar spinal cord of a P60 *Y1::EGFP; NPY::Cre* transgenic mouse. Presynaptic contacts (red) from NPY::Cre INs onto Y1/EGFP^{+} cells were visualized with a Cre-dependent AAV2/1-hSyn-DIO-SypHTom virus. Putative synaptic boutons marked by VGAT (blue; A) and NPY (blue; B) immunoreactivity are indicated by arrowheads.

(C) Examples of synaptic puncta labeled with antibodies against NPY (green) and gephyrin (blue) on a Y1-tdTomato^{+} cell body in the lumbar spinal cord of a P42 *Y1^{Cre}; Ai14$^{lsl\text{-}tdTom}$* mouse (arrowheads).

(D) Schematic illustrating experimental conditions used to assess synaptic connectivity between NPY::Cre INs and Y1^{Cre} neurons.

(E) ReaChR-mediated activation of NPY::Cre IN generated monosynaptic outward currents in lamina IIi Y1-EGFP^{+} neurons in P14-21 *Y1::EGFP; NPY::Cre; Lbx1^{FlpO}; R26$^{ds\text{-}ReaChR}$* spinal cord slices in the presence of kynurenic acid (KA; 1.5 mM) at a holding potential of −30 mV. These currents were abolished following application of 1 μM strychnine and 60 μM picrotoxin (n = 7 cells from 5 mice). ***p < 0.001. The statistical difference was determined by the two-tailed, paired t test.

(F) Traces recorded from a Y1-EGFP^{+} neuron showing a monosynaptic inhibitory current elicited by NPY::Cre activation (purple trace) and no response following bath application of strychnine and picrotoxin (black trace).

Scale bars: 5 μm.

The role of Y1 signaling in the regulation of mechanical itch was further assessed by administering NPY or the selective Y1 agonist [Leu^{31}, Pro^{34}]-NPY (Gelfo et al., 2011) to *NPY::Cre*; *Lbx1^{FlpO}*; *Tau$^{ds\text{-}DTR}$*; *Ai65$^{ds\text{-}tdTom}$* mice 1 week after ablating the NPY::Cre INs. Both agonists relieved spontaneous scratching in the NPY::Cre IN-ablated mice (Figures 7A and S7D). Furthermore, injection of NPY (Figure S7E) or [Leu^{31}, Pro^{34}]-NPY reduced sensitivity to nape stimulation, with this effect being abolished when [Leu^{31}, Pro^{34}]-NPY was administered to *Lbx1^{Cre}*; *Y1$^{f/f}$* mice, confirming the dorsal horn as the site of NPY action (Figures 7B and S7F).

As a final test of the functional interaction between the NPY::Cre and Y1^{+} neurons, we assessed itch sensitivity following chemogenetic activation of NPY::Cre INs. When NPY::Cre INs were selectively activated, evoked scratching was reduced compared to controls (Figure 7C). This reduction in scratching was negated by co-injecting BIBP 3226 with CNO, indicating that the inhibition of itch by NPY::Cre INs is in large part dependent on the actions of NPY on the Y1^{+} neurons (Figure 7D). Importantly, the inhibition of itch by NPY::Cre IN activation was specific to mechanical itch, as chloroquine-induced scratching was unaffected (Figure 7E).

The activation of NPY::Cre INs also caused a pronounced reduction in the sensitivity of the glabrous skin to light punctate touch, as well as more moderate reductions in responses to dynamic touch and acute pain (Figures 7F–7H). These effects were not observed when BIBP 3226 was administered (Figures 7I–7K), implying that they were mediated by enhanced release of NPY. Given that dorsal horn Y1^{+} neurons do not transmit dynamic touch and acute pain, it is likely that the modulation of these modalities following NPY::Cre IN activation results from ectopic activation of Y1 receptors expressed by sensory neurons. Taken together, these data support a model in which light punctate touch and mechanical itch are strongly regulated by

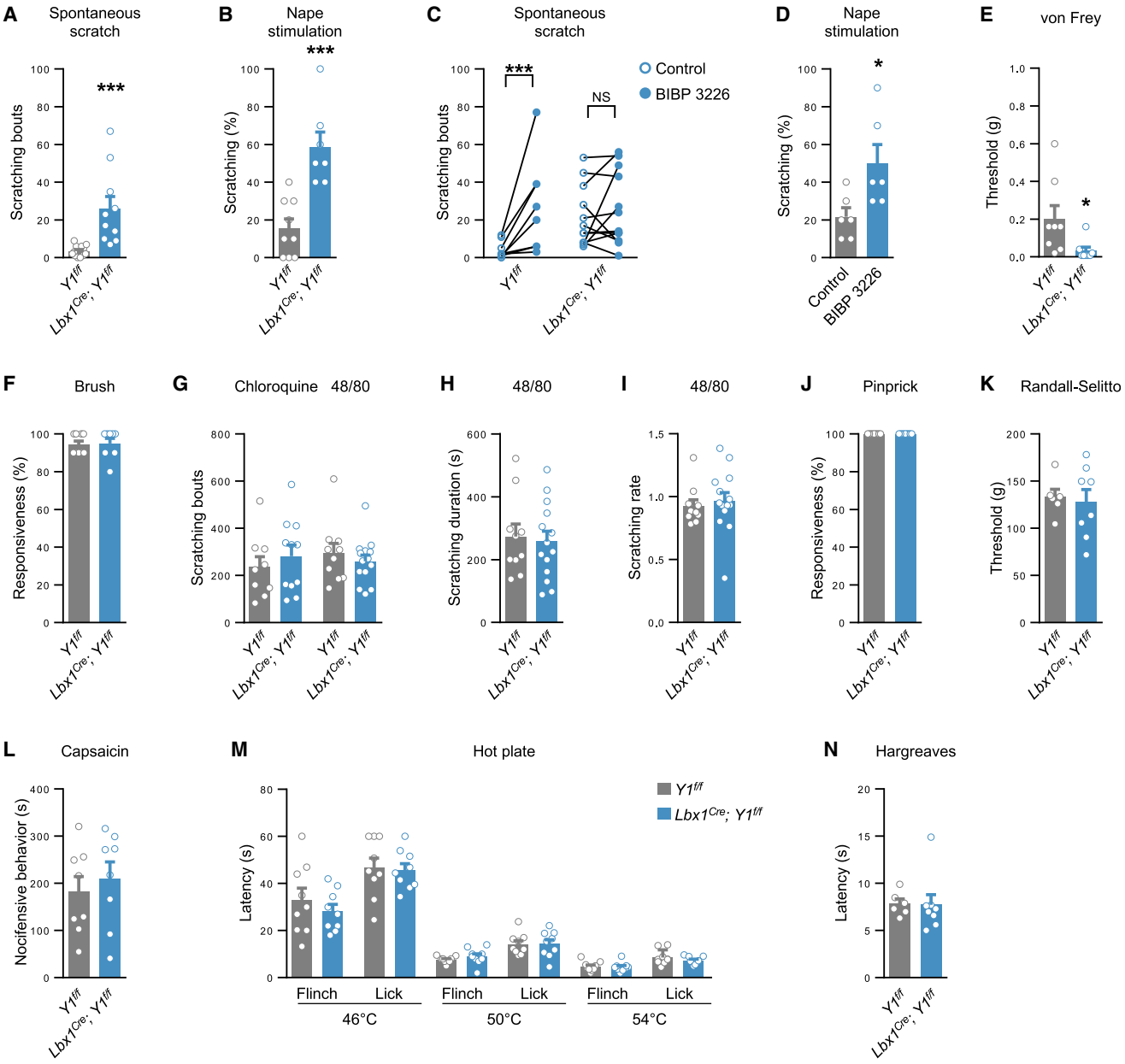

Figure 6. NPY-Y1 Receptor Signaling within the Dorsal Horn Gates Mechanical Itch and Light Punctate Touch

(A and B) Mice lacking the Y1 receptor in dorsal horn neurons exhibit pronounced spontaneous scratching (A; *Lbx1*^{Cre}*; Y1*$^{f/f}$, n = 10; *Y1*$^{f/f}$ control, n = 12) and hypersensitivity to light punctate mechanical stimulation of the nape (B; *Lbx1*^{Cre}*; Y1*$^{f/f}$, n = 7; *Y1*$^{f/f}$ control, n = 9).

(C) The Y1 antagonist BIBP 3226 (1 mg kg^{-1}, intraperitoneally [i.p.]) increases spontaneous scratching in control (n = 8) but not conditional knockout mice (n = 12). Two-tailed, paired t tests were used to assess statistical differences.

(D) BIBP 3226 causes hypersensitivity to nape stimulation (n = 12; vehicle, n = 12).

(E and F) *Lbx1*^{Cre}; *Y1*$^{f/f}$ mice have reduced hindpaw von Frey thresholds (E; *Lbx1*^{Cre}*; Y1*$^{f/f}$, n = 8; *Y1*$^{f/f}$ control, n = 8) but responses to dynamic touch are unaltered (F; *Lbx1*^{Cre}*; Y1*$^{f/f}$, n = 8; *Y1*$^{f/f}$ control, n = 9).

(G–I) Deletion of Y1 from dorsal horn neurons does not alter scratching frequency in response to chloroquine (*Lbx1*^{Cre}*; Y1*$^{f/f}$, n = 11; *Y1*$^{f/f}$ control, n = 9) or scratching frequency (G), duration (H), or rate (duration/frequency; I) in response to compound 48/80 (*Lbx1*^{Cre}*; Y1*$^{f/f}$, n = 14; *Y1*$^{f/f}$ control, n = 10).

(J–N) Deletion of Y1 from dorsal horn neurons does not affect sensitivity to acute mechanical pain as assessed by pinprick (J; *Lbx1*^{Cre}*; Y1*$^{f/f}$, n = 9; *Y1*$^{f/f}$ control, n = 9) or the Randall-Selitto test (K; *Lbx1*^{Cre}*; Y1*$^{f/f}$, n = 8; *Y1*$^{f/f}$ control, n = 6), chemical nociception (L; *Lbx1*^{Cre}*; Y1*$^{f/f}$, n = 8; *Y1*$^{f/f}$ control, n = 8), or thermal pain as assessed by the hot plate (M; *Lbx1*^{Cre}*; Y1*$^{f/f}$, n = 9; *Y1*$^{f/f}$ control, n = 9) or Hargreaves tests (N; *Lbx1*^{Cre}*; Y1*$^{f/f}$, n = 8; *Y1*$^{f/f}$ control, n = 6).

*p < 0.05 and ***p < 0.001. NS, not significant. Data: mean ± SEM.

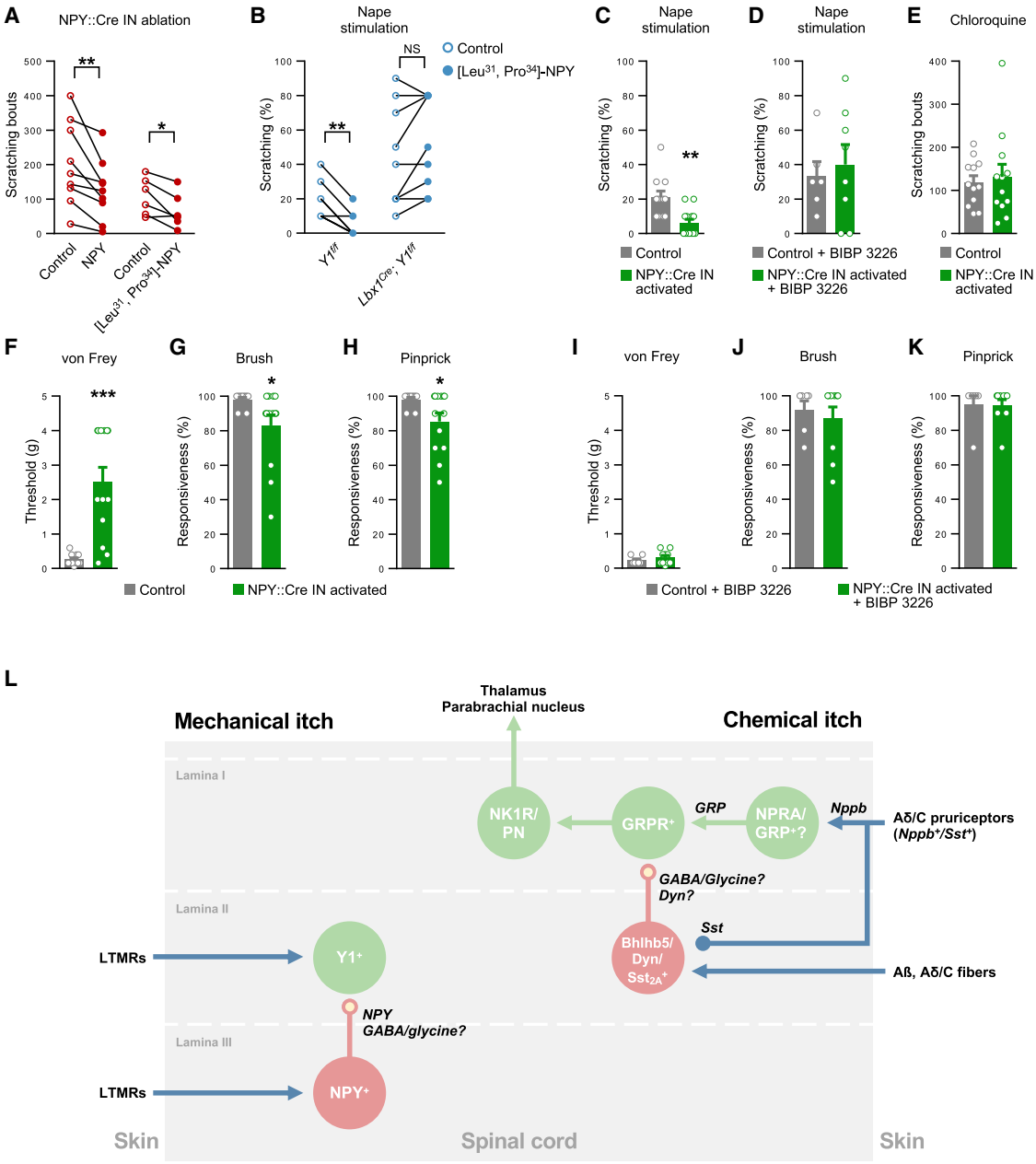

Figure 7. NPY-Y1 Receptor Signaling Determines Sensitivity to Mechanical Itch Stimuli

(A) Spontaneous scratching in *NPY::Cre; Lbx1*^{FlpO}*; Tau*$^{ds\text{-}DTR}$*; Ai65*$^{ds\text{-}tdTom}$ mice 1 week after DT treatment was reduced following injection of NPY (100 μg kg^{-1}, i.p.; n = 9) or the selective Y1 receptor agonist [Leu^{31}, Pro^{34}]-NPY (100 μg kg^{-1}, i.p.; n = 6) when compared with vehicle.

(B) Evoked scratching is reduced when *Y1*$^{f/f}$ mice (n = 8) but not *Lbx1*^{Cre}*; Y1*$^{f/f}$ mice (n = 9) are injected with [Leu^{31}, Pro^{34}]-NPY (100 μg kg^{-1}, i.p., n = 8; vehicle, n = 8).

(C and D) hM3D-mediated activation of the NPY::Cre INs reduces scratching in response to mechanical stimulation of the nape compared with controls (*NPY::Cre; Lbx1*^{FlpO}*; R26*$^{ds\text{-}hM3D}$, n = 13; *NPY::Cre; R26*$^{ds\text{-}hM3D}$ controls, n = 11; C) but not when Y1 receptors are inhibited by BIBP 3226 (n = 7; controls, n = 9; D).

(E) Unchanged chloroquine-induced scratching following activation of the NPY::Cre INs (n = 12; controls, n = 12).

(F–H) Activation of NPY::Cre INs reduces sensitivity to von Frey hair (F), brush (G), and pinprick (H) stimulation of the plantar hindpaw (n = 13; controls, n = 11).

(I–K) Activation of NPY::Cre INs does not alter sensitivity to von Frey hair (I), brush (J), and pinprick (K) stimulation following Y1 receptor blockade by BIBP 3226 (n = 9; BIBP 3226-injected controls, n = 7).

(L) Schematic showing proposed dorsal horn circuitry for mechanical and chemical itch. Dyn, dynorphin; Nppb, natriuretic peptide B; NPRA, natriuretic peptide receptor A; PN, projection neuron; Sst_{2A}, Sst 2A receptor. Italics indicate neurotransmitters/neuropeptides.

Two-tailed, paired (A and B) or unpaired (C–K) t tests were used to assess statistical differences. *p < 0.05, **p < 0.01, ***p < 0.001. NS, not significant. Data: mean ± SEM (B–L). See also Figure S7.

the actions of NPY on inhibitory Y1-bearing neurons in the dorsal horn.

DISCUSSION

In this study we have identified the population of excitatory neurons in the dorsal spinal cord that are essential for transmitting the mechanosensory stimuli that drive mechanical itch. These neurons are marked by Y1 receptor expression and they define, together with NPY::Cre inhibitory INs in the dorsal horn, a central pathway for mechanical itch transmission that is distinct from the well-described GRP-GRPR chemical itch pathway (Figure 7L). Scratching in response to mechanical stimulation is abolished when the $Y1^{Cre}$ neurons are ablated, while activation of the $Y1^{Cre}$ neurons increases scratching in response to mechanical stimulation. Our results also reveal a prominent role for NPY peptidergic signaling in regulating light punctate touch sensitivity and mechanical itch, which is mediated by $Y1^{+}$ neurons in the dorsal horn. We propose that NPY inhibitory signaling normally facilitates the discrimination of light touch stimuli, and disrupting it promotes a chronic itch phenotype and mechanical hyperknesis/alloknesis.

Dorsal Horn $Y1^{Cre}$ Neurons Transmit Low-Threshold Mechanical Stimuli

The light punctate touch and mechanical itch phenotypes we observe upon manipulation of the $Y1^{Cre}$ neurons are consistent with their innervation by mechanosensory LTMR afferents from both the glabrous and hairy skin (Figure 2). Whereas the $Y1^{Cre}$ neurons encompass multiple cell types within the LTMR-RZ (Figures S2 and S3), our findings suggest that only a subset of these cells are required for mechanical itch responses, and this subset appears to be distinct from those $Y1^{Cre}$ neurons that express Sst or NK1R, as ablating the Sst^{+} or $NK1R^{+}$ neurons fails to disrupt the mechanical itch pathway (Figures 3 and S5).

Touch information appears to be broadly distributed between overlapping molecularly defined populations within the LTMR-RZ that include $Y1^{+}$, $ROR\alpha^{+}$, Sst^{+}, $vGlut3^{+}$, and $calretinin^{+}$ neurons (this study; Abraira et al., 2017; Abraira and Ginty, 2013; Bourane et al., 2015b; Duan et al., 2014; Peirs et al., 2015). Interestingly, the role of the $Y1^{+}$ neurons in processing touch information appears to be limited to punctuate touch, since they are dispensable for transmitting dynamic light touch information (Figure 3), which is instead largely transmitted by excitatory $ROR\alpha^{+}$ INs in laminae IIi/III (Bourane et al., 2015b). The contribution that dynamic touch and the $RORa^{+}$ INs make to mechanical itch is still unclear.

The possibility that the $Y1^{Cre}$ neurons may contribute to the transmission of other cutaneous modalities is suggested by our observation that some $Y1^{Cre}$ neurons reside in laminae I–IIo, subsets of which are Sst^{+} neurons, which have been implicated in acute mechanical pain and lamina I $NK1R^{+}$ neurons, which transmit chemical pain (Brumovsky et al., 2002; Duan et al., 2014; Mantyh et al., 1997; Nichols et al., 1999). Somewhat surprisingly, our functional analyses did not reveal a role for the $Y1^{Cre}$ neurons in acute mechanical pain or responses to noxious heat or chemical stimuli (Figure 4). Moreover, the absence of a pain phenotype following $Y1^{Cre}$ neuron ablation or activation suggests the $Y1^{Cre}/Sst^{Cre}$ and $Y1^{Cre}/NK1R^{+}$ neurons are dispensable for pain transmission.

Chemical itch transmission was also unaffected following ablation of the $Y1^{Cre}$ neurons (Figure 3), with this study and our previous functional analysis of the NPY::Cre INs (Bourane et al., 2015a) providing strong evidence that the pathways for mechanical and chemical itch are largely segregated in the periphery and dorsal spinal cord (Figures 3 and 7L). Although the $Y1^{Cre}$ population partially overlaps with $NK1R^{+}$, Sst^{+}, and GRP^{+} neurons that have been implicated in chemical itch transmission (Albisetti et al., 2019; Christensen et al., 2016; Fatima et al., 2019; Huang et al., 2018; Kardon et al., 2014; Mishra and Hoon, 2013), those embedded within the $Y1^{Cre}$ population appear to be dispensable for chemical itch.

Mechanical and chemical itch stimuli produce indistinguishable sensations in humans, and both trigger scratching (Fukuoka et al., 2013). This suggests central convergence of the mechanical and chemical itch pathways, a possibility supported by observations that chemical pruritogens can cause alloknesis, a condition in which normally innocuous mechanical stimuli cause itch (Akiyama et al., 2012; Gao et al., 2018; Wahlgren et al., 1991). Moreover, there is evidence that the parabrachial nucleus (Campos et al., 2018; Mu et al., 2017) to which $NK1R^{+}$ neurons project (Akiyama et al., 2015) encodes both mechanical and chemical itch. Our results show that the $NK1R^{+}$ neurons are dispensable for mechanical itch, which suggests that the chemical and mechanical itch pathways do not converge in the spinal cord on ascending $NK1R^{+}$ projection neurons.

NPY-Y1R Signaling Gates Mechanical Itch

Our analysis reveals a key role for NPY in regulating mechanical itch and touch sensitivity. We propose that NPY-Y1 signaling functions in healthy animals as a homeostatic mechanism to adjust the output of the LTMR circuitry, thus ensuring the correct discrimination between itch and other innocuous light touch sensations. Recently, it has been reported that NPY suppresses itch (Gao et al., 2018), although the site of action and the cellular basis for this activity were not described. Our studies show endogenous NPY acts on $Y1^{+}$ neurons in the dorsal horn to regulate mechanical itch, the same cells that are required for the chronic itch phenotype in NPY::Cre IN ablated mice (Figure 3). We cannot completely exclude the possibility that NPY-Y1 signaling in sensory afferents also contributes to the modulation of mechanosensory transmission; however, this is unlikely, as in these neurons Y1 is co-expressed with CGRP (Brumovsky et al., 2002), a marker of high-threshold mechanoreceptors (Lawson et al., 2002).

While our results show the inhibitory effects of NPY::Cre IN activation are largely abolished by Y1 blockade, the present study does not eliminate a role for GABA or glycine in the regulation of the mechanical itch pathway. Rather, Y1-mediated inhibition may operate in conjunction with fast inhibitory pathways (Akiyama et al., 2011; Ralvenius et al., 2018) to regulate the sensitivity of the dorsal horn mechanosensory circuitry over longer time scales than those controlled by ionotropic feedforward inhibition. It is also possible that peptidergic signaling between NPY::Cre and $Y1^{+}$ neurons contributes to the inhibition of mechanical itch by counterstimuli, a role that would be consistent with our observation that after-discharge

spiking is enhanced following brushing of the hairy skin in NPY::-Cre IN-ablated mice (Bourane et al., 2015a).

The central inhibition of mechanical itch by NPY::Cre INs parallels the inhibitory regulation of chemical itch by the B5-I INs (Figure 7L) (Chiang et al., 2016; Kardon et al., 2014; Ross et al., 2010). B5-I INs are a subset of lamina I-II inhibitory INs that express the transcription factor Bhlhb5. These cells suppress activity in a tonic manner (Huang et al., 2018; Kardon et al., 2014; Ross et al., 2010) and in response to counterstimuli (Hachisuka et al., 2016; Kardon et al., 2014). The B5-I INs include the spinal INs that express the neuropeptide dynorphin, the endogenous agonist of kappa opioid receptors, and as in mechanical itch, a neuropeptidergic mechanism is proposed to regulate the chemical itch pathway in a tonic manner (Huang et al., 2018; Kardon et al., 2014; however, also see Duan et al., 2014).

Several studies have found that NPY exerts analgesic effects via two of the five identified mammalian NPY receptors, the Y1 and Y2 receptors, in neuropathic, inflammatory, and some forms of acute pain (Diaz-delCastillo et al., 2018; Duggan et al., 1991; Hua et al., 1991; Intondi et al., 2008; Naveilhan et al., 2001; Solway et al., 2011; Taiwo and Taylor 2002). Y1 signaling is also required for normal sensitivity to heat (Naveilhan et al., 2001). However, it was previously unclear whether these effects are mediated by central or peripheral mechanisms (Diaz-delCastillo et al., 2018; Gibbs et al., 2004; Moran et al., 2004). We find that ablation of $Y1^{Cre}$ neurons or deletion of the *Y1* gene within the dorsal horn has no effect on acute, thermal, or chemical nociception (Figure 4), strongly indicating that they are instead mediated by peptidergic $Y1^{+}$ nociceptive afferents (Brumovsky et al., 2002), rather than $Y1^{+}$ neurons in the dorsal horn. This finding further suggests that the mild Y1-dependent inhibition of acute pain and dynamic touch observed following activation of the NPY::Cre INs (Figure 7) entails ectopic inhibition of $Y1^{+}$ primary afferents, and that other inhibitory neurons play a more prominent role in gating these modalities under physiological conditions.

In summary, this study demonstrates that $Y1^{+}$ neurons form an excitatory pathway within the dorsal horn for the transmission of mechanical itch, and that the flow of information through this pathway is regulated by inhibitory NPY-Y1 signaling to maintain normal touch discrimination. We propose that dysregulation of this pathway following failure of the gating mechanism may drive the development of neuropathic chronic itch. It has been suggested that increases in mechanical itch sensitivity in mice following the loss of Merkel cells due to aging or dry skin might be due to reduced cutaneous input to inhibitory NPY-expressing INs, although this has not been tested (Feng et al., 2018). There is also evidence that the disruption of NPY signaling in humans may contribute to chronic itch (Reich et al., 2013). Notably, psoriasis patients presenting with pruritus have reduced NPY serum levels, which are negatively correlated with the intensity of itch (Reich et al., 2007). In view of the central contribution NPY signaling makes to the inhibitory regulation of itch sensation, Y1 signaling merits investigation as a therapeutic target for the treatment of chronic itch, a condition that rivals chronic pain in the severity of its impact on quality of life (Kini et al., 2011).

STAR★METHODS

Detailed methods are provided in the online version of this paper and include the following:

- KEY RESOURCES TABLE
- LEAD CONTACT AND MATERIALS AVAILABILITY
- EXPERIMENTAL MODEL AND SUBJECT DETAILS
- METHOD DETAILS
  - Immunohistochemistry
  - *In Situ* Hybridization
  - Rabies Virus Tracing and Morphological Analyses
  - AAV Virus Tracing of Synaptic Connections
  - Retrograde Cholera Toxin-b Labeling of Cutaneous Sensory Neurons
  - Cell Ablation
  - Drug Administration
  - Electrophysiology
  - Behavioral Testing
- QUANTIFICATION AND STATISTICAL ANALYSIS

SUPPLEMENTAL INFORMATION

Supplemental Information can be found online at https://doi.org/10.1016/j.celrep.2019.06.033.

ACKNOWLEDGMENTS

This study was supported by grants from the NIH (NS0850586, NS086372, and NS111643 to M.G.) and by the Caterina Foundation (D.A.). Synthesis of [Leu^{31}, Pro^{34}]-NPY was supported by the Peptide Synthesis and Proteomics Core Facilities of the Salk Institute with funding from NIH-NCI CCSG (P30 014195). Rabies viruses were generated and kindly provided by Kim Ritola, HHMI Janelia. M.G. holds the Frederick and Joanne Mitchell Chair at the Salk Institute. We thank Qiufu Ma for insightful comments on the manuscript.

AUTHOR CONTRIBUTIONS

D.A., S.D.C., X.R., A.D., S.B., and M.G. all contributed to the experimental analyses. I.B. and C.E. generated the Y1 receptor conditional mutant mice that were used in this study. D.A. and M.G. designed the experiments and wrote the manuscript.

DECLARATION OF INTERESTS

The authors declare no competing interests.

Received: October 11, 2018
Revised: May 20, 2019
Accepted: June 6, 2019
Published: July 16, 2019

REFERENCES

Abraira, V.E., and Ginty, D.D. (2013). The sensory neurons of touch. Neuron *79*, 618–639.

Abraira, V.E., Kuehn, E.D., Chirila, A.M., Springel, M.W., Toliver, A.A., Zimmerman, A.L., Orefice, L.L., Boyle, K.A., Bai, L., Song, B.J., et al. (2017). The Cellular and Synaptic Architecture of the Mechanosensory Dorsal Horn. Cell *168*, 295–310.e19.

Akiyama, T., Iodi Carstens, M., and Carstens, E. (2011). Transmitters and pathways mediating inhibition of spinal itch-signaling neurons by scratching and other counterstimuli. PLoS ONE *6*, e22665.

Akiyama, T., Carstens, M.I., Ikoma, A., Cevikbas, F., Steinhoff, M., and Carstens, E. (2012). Mouse model of touch-evoked itch (alloknesis). J. Invest. Dermatol. *132*, 1886–1891.

Akiyama, T., Tominaga, M., Davoodi, A., Nagamine, M., Blansit, K., Horwitz, A., Carstens, M.I., and Carstens, E. (2013). Roles for substance P and gastrin-releasing peptide as neurotransmitters released by primary afferent pruriceptors. J. Neurophysiol. *109*, 742–748.

Akiyama, T., Nguyen, T., Curtis, E., Nishida, K., Devireddy, J., Delahanty, J., Carstens, M.I., and Carstens, E. (2015). A central role for spinal dorsal horn neurons that express neurokinin-1 receptors in chronic itch. Pain *156*, 1240–1246.

Albisetti, G.W., Ghanem, A., Foster, E., Conzelmann, K.-K., Zeilhofer, H.U., and Wildner, H. (2017). Identification of two classes of somatosensory neurons that display resistance to retrograde infection by rabies virus. J. Neurosci. *37*, 10358–10371.

Albisetti, G.W., Pagani, M., Platonova, E., Hösli, L., Johannssen, H.C., Fritschy, J.-M., Wildner, H., and Zeilhofer, H.U. (2019). Dorsal Horn Gastrin-Releasing Peptide Expressing Neurons Transmit Spinal Itch But Not Pain Signals. J. Neurosci. *39*, 2238–2250.

Antal-Zimanyi, I., Bruce, M.A., Leboulluec, K.L., Iben, L.G., Mattson, G.K., McGovern, R.T., Hogan, J.B., Leahy, C.L., Flowers, S.C., Stanley, J.A., et al. (2008). Pharmacological characterization and appetite suppressive properties of BMS-193885, a novel and selective neuropeptide Y(1) receptor antagonist. Eur. J. Pharmacol. *590*, 224–232.

Bautista, D.M., Wilson, S.R., and Hoon, M.A. (2014). Why we scratch an itch: the molecules, cells and circuits of itch. Nat. Neurosci. *17*, 175–182.

Bertocchi, I., Oberto, A., Longo, A., Mele, P., Sabetta, M., Bartolomucci, A., Palanza, P., Sprengel, R., and Eva, C. (2011). Regulatory functions of limbic Y1 receptors in body weight and anxiety uncovered by conditional knockout and maternal care. Proc. Natl. Acad. Sci. USA *108*, 19395–19400.

Bourane, S., Duan, B., Koch, S.C., Dalet, A., Britz, O., Garcia-Campmany, L., Kim, E., Cheng, L., Ghosh, A., Ma, Q., and Goulding, M. (2015a). Gate control of mechanical itch by a subpopulation of spinal cord interneurons. Science *350*, 550–554.

Bourane, S., Grossmann, K.S., Britz, O., Dalet, A., Del Barrio, M.G., Stam, F.J., Garcia-Campmany, L., Koch, S., and Goulding, M. (2015b). Identification of a spinal circuit for light touch and fine motor control. Cell *160*, 503–515.

Britz, O., Zhang, J., Grossmann, K.S., Dyck, J., Kim, J.C., Dymecki, S., Gosgnach, S., and Goulding, M. (2015). A genetically defined asymmetry underlies the inhibitory control of flexor-extensor locomotor movements. eLife *4*, e04718.

Brumovsky, P.R., Shi, T.J., Matsuda, H., Kopp, J., Villar, M.J., and Hökfelt, T. (2002). NPY Y1 receptors are present in axonal processes of DRG neurons. Exp. Neurol. *174*, 1–10.

Brumovsky, P., Hofstetter, C., Olson, L., Ohning, G., Villar, M., and Hökfelt, T. (2006). The neuropeptide tyrosine Y1R is expressed in interneurons and projection neurons in the dorsal horn and area X of the rat spinal cord. Neuroscience *138*, 1361–1376.

Campos, C.A., Bowen, A.J., Roman, C.W., and Palmiter, R.D. (2018). Encoding of danger by parabrachial CGRP neurons. Nature *555*, 617–622.

Carstens, E.E., Carstens, M.I., Simons, C.T., and Jinks, S.L. (2010). Dorsal horn neurons expressing NK-1 receptors mediate scratching in rats. Neuroreport *21*, 303–308.

Chaplan, S.R., Bach, F.W., Pogrel, J.W., Chung, J.M., and Yaksh, T.L. (1994). Quantitative assessment of tactile allodynia in the rat paw. J. Neurosci. Methods *53*, 55–63.

Chiang, M.C., Hachisuka, J., Todd, A.J., and Ross, S.E. (2016). Insight into B5-I spinal interneurons and their role in the inhibition of itch and pain. Pain *157*, 544–545.

Christensen, A.J., Iyer, S.M., François, A., Vyas, S., Ramakrishnan, C., Vesuna, S., Deisseroth, K., Scherrer, G., and Delp, S.L. (2016). In Vivo Interrogation of Spinal Mechanosensory Circuits. Cell Rep. *17*, 1699–1710.

Davidson, S., Zhang, X., Yoon, C.H., Khasabov, S.G., Simone, D.A., and Giesler, G.J., Jr. (2007). The itch-producing agents histamine and cowhage activate separate populations of primate spinothalamic tract neurons. J. Neurosci. *27*, 10007–10014.

Davidson, S., Zhang, X., Khasabov, S.G., Moser, H.R., Honda, C.N., Simone, D.A., and Giesler, G.J., Jr. (2012). Pruriceptive spinothalamic tract neurons: physiological properties and projection targets in the primate. J. Neurophysiol. *108*, 1711–1723.

Diaz-delCastillo, M., Woldbye, D.P.D., and Heegaard, A.M. (2018). Neuropeptide Y and its Involvement in Chronic Pain. Neuroscience *387*, 162–169.

Dong, X., and Dong, X. (2018). Peripheral and Central Mechanisms of Itch. Neuron *98*, 482–494.

Duan, B., Cheng, L., Bourane, S., Britz, O., Padilla, C., Garcia-Campmany, L., Krashes, M., Knowlton, W., Velasquez, T., Ren, X., et al. (2014). Identification of spinal circuits transmitting and gating mechanical pain. Cell *159*, 1417–1432.

Duggan, A.W., Hope, P.J., and Lang, C.W. (1991). Microinjection of neuropeptide Y into the superficial dorsal horn reduces stimulus-evoked release of immunoreactive substance P in the anaesthetized cat. Neuroscience *44*, 733–740.

Fatima, M., Ren, X., Pan, H., Slade, H.F.E., Asmar, A.J., Xiong, C.M., Shi, A., Xiong, A.E., Wang, L., and Duan, B. (2019). Spinal somatostatin-positive interneurons transmit chemical itch. Pain *160*, 1166–1174.

Feng, J., Luo, J., Yang, P., Du, J., Kim, B.S., and Hu, H. (2018). Piezo2 channel-Merkel cell signaling modulates the conversion of touch to itch. Science *360*, 530–533.

Fuhlendorff, J., Gether, U., Aakerlund, L., Langeland-Johansen, N., Thøgersen, H., Melberg, S.G., Olsen, U.B., Thastrup, O., and Schwartz, T.W. (1990). [Leu31, Pro34]neuropeptide Y: a specific Y1 receptor agonist. Proc. Natl. Acad. Sci. USA *87*, 182–186.

Fukuoka, M., Miyachi, Y., and Ikoma, A. (2013). Mechanically evoked itch in humans. Pain *154*, 897–904.

Gao, T., Ma, H., Xu, B., Bergman, J., Larhammar, D., and Lagerström, M.C. (2018). The Neuropeptide Y System Regulates Both Mechanical and Histaminergic Itch. J. Invest. Dermatol. *138*, 2405–2411.

Gelfo, F., De Bartolo, P., Tirassa, P., Croce, N., Caltagirone, C., Petrosini, L., and Angelucci, F. (2011). Intraperitoneal injection of neuropeptide Y (NPY) alters neurotrophin rat hypothalamic levels: Implications for NPY potential role in stress-related disorders. Peptides *32*, 1320–1323.

Gibbs, J., Flores, C.M., and Hargreaves, K.M. (2004). Neuropeptide Y inhibits capsaicin-sensitive nociceptors via a Y1-receptor-mediated mechanism. Neuroscience *125*, 703–709.

Grudt, T.J., and Perl, E.R. (2002). Correlations between neuronal morphology and electrophysiological features in the rodent superficial dorsal horn. J. Physiol. *540*, 189–207.

Hachisuka, J., Baumbauer, K.M., Omori, Y., Snyder, L.M., Koerber, H.R., and Ross, S.E. (2016). Semi-intact ex vivo approach to investigate spinal somatosensory circuits. eLife *5*, e22866.

Hachisuka, J., Chiang, M.C., and Ross, S.E. (2018). Itch and neuropathic itch. Pain *159*, 603–609.

Han, L., and Dong, X. (2014). Itch mechanisms and circuits. Annu. Rev. Biophys. *43*, 331–355.

Häring, M., Zeisel, A., Hochgerner, H., Rinwa, P., Jakobsson, J.E.T., Lönnerberg, P., La Manno, G., Sharma, N., Borgius, L., Kiehn, O., et al. (2018). Neuronal atlas of the dorsal horn defines its architecture and links sensory input to transcriptional cell types. Nat. Neurosci. *21*, 869–880.

He, M., Tucciarone, J., Lee, S., Nigro, M.J., Kim, Y., Levine, J.M., Kelly, S.M., Krugikov, I., Wu, P., Chen, Y., et al. (2016). Strategies and Tools for Combinatorial Targeting of GABAergic Neurons in Mouse Cerebral Cortex. Neuron *91*, 1228–1243.

Hooks, B.M., Lin, J.Y., Guo, C., and Svoboda, K. (2015). Dual-channel circuit mapping reveals sensorimotor convergence in the primary motor cortex. J. Neurosci. *35*, 4418–4426.

Hua, X.Y., Boublik, J.H., Spicer, M.A., Rivier, J.E., Brown, M.R., and Yaksh, T.L. (1991). The antinociceptive effects of spinally administered neuropeptide Y in the rat: systematic studies on structure-activity relationship. J. Pharmacol. Exp. Ther. *258*, 243–248.

Huang, J., Polgár, E., Solinski, H.J., Mishra, S.K., Tseng, P.-Y., Iwagaki, N., Boyle, K.A., Dickie, A.C., Kriegbaum, M.C., Wildner, H., et al. (2018). Circuit dissection of the role of somatostatin in itch and pain. Nat. Neurosci. *21*, 707–716.

Ikoma, A. (2013). Updated neurophysiology of itch. Biol. Pharm. Bull. *36*, 1235–1240.

Ikoma, A., Steinhoff, M., Ständer, S., Yosipovitch, G., and Schmelz, M. (2006). The neurobiology of itch. Nat. Rev. Neurosci. *7*, 535–547.

Intondi, A.B., Dahlgren, M.N., Eilers, M.A., and Taylor, B.K. (2008). Intrathecal neuropeptide Y reduces behavioral and molecular markers of inflammatory or neuropathic pain. Pain *137*, 352–365.

Jacques, D., Cadieux, A., Dumont, Y., and Quirion, R. (1995). Apparent affinity and potency of BIBP3226, a non-peptide neuropeptide Y receptor antagonist, on purported neuropeptide Y Y1, Y2 and Y3 receptors. Eur. J. Pharmacol. *278*, R3–R5.

Jensen, E.C. (2013). Quantitative analysis of histological staining and fluorescence using ImageJ. Anat. Rec. (Hoboken) *296*, 378–381.

Johanek, L.M., Meyer, R.A., Friedman, R.M., Greenquist, K.W., Shim, B., Borzan, J., Hartke, T., LaMotte, R.H., and Ringkamp, M. (2008). A role for polymodal C-fiber afferents in nonhistaminergic itch. J. Neurosci. *28*, 7659–7669.

Kardon, A.P., Polgár, E., Hachisuka, J., Snyder, L.M., Cameron, D., Savage, S., Cai, X., Karnup, S., Fan, C.R., Hemenway, G.M., et al. (2014). Dynorphin acts as a neuromodulator to inhibit itch in the dorsal horn of the spinal cord. Neuron *82*, 573–586.

Karl, T., Duffy, L., and Herzog, H. (2008). Behavioural profile of a new mouse model for NPY deficiency. Eur. J. Neurosci. *28*, 173–180.

Kini, S.P., DeLong, L.K., Veledar, E., McKenzie-Brown, A.M., Schaufele, M., and Chen, S.C. (2011). The impact of pruritus on quality of life: the skin equivalent of pain. Arch. Dermatol. *147*, 1153–1156.

Koch, S.C., Del Barrio, M.G., Dalet, A., Gatto, G., Günther, T., Zhang, J., Seidler, B., Saur, D., Schüle, R., and Goulding, M. (2017). RORβ Spinal Interneurons Gate Sensory Transmission during Locomotion to Secure a Fluid Walking Gait. Neuron *96*, 1419–1431.e5.

Koch, S.C., Acton, D., and Goulding, M. (2018). Spinal Circuits for Touch, Pain, and Itch. Annu. Rev. Physiol. *80*, 189–217.

Lawson, S.N., Crepps, B., and Perl, E.R. (2002). Calcitonin gene-related peptide immunoreactivity and afferent receptive properties of dorsal root ganglion neurones in guinea-pigs. J. Physiol. *540*, 989–1002.

Ma, C., Nie, H., Gu, Q., Sikand, P., and Lamotte, R.H. (2012). In vivo responses of cutaneous C-mechanosensitive neurons in mouse to punctate chemical stimuli that elicit itch and nociceptive sensations in humans. J. Neurophysiol. *107*, 357–363.

Madisen, L., Zwingman, T.A., Sunkin, S.M., Oh, S.W., Zariwala, H.A., Gu, H., Ng, L.L., Palmiter, R.D., Hawrylycz, M.J., Jones, A.R., et al. (2010). A robust and high-throughput Cre reporting and characterization system for the whole mouse brain. Nat. Neurosci. *13*, 133–140.

Madisen, L., Garner, A.R., Shimaoka, D., Chuong, A.S., Klapoetke, N.C., Li, L., van der Bourg, A., Niino, Y., Egolf, L., Monetti, C., et al. (2015). Transgenic mice for intersectional targeting of neural sensors and effectors with high specificity and performance. Neuron *85*, 942–958.

Mantyh, P.W., Rogers, S.D., Honore, P., Allen, B.J., Ghilardi, J.R., Li, J., Daughters, R.S., Lappi, D.A., Wiley, R.G., and Simone, D.A. (1997). Inhibition of hyperalgesia by ablation of lamina I spinal neurons expressing the substance P receptor. Science *278*, 275–279.

Melnick, I.V. (2012). Cell type-specific postsynaptic effects of neuropeptide Y in substantia gelatinosa neurons of the rat spinal cord. Synapse *66*, 640–649.

Mishra, S.K., and Hoon, M.A. (2013). The cells and circuitry for itch responses in mice. Science *340*, 968–971.

Miyakawa, A., Furue, H., Katafuchi, T., Jiang, N., Yasaka, T., Kato, G., and Yoshimura, M. (2005). Action of neuropeptide Y on nociceptive transmission in substantia gelatinosa of the adult rat spinal dorsal horn. Neuroscience *134*, 595–604.

Moran, T.D., Colmers, W.F., and Smith, P.A. (2004). Opioid-Like Actins of Neuropeptide Y in Rat Substantia Gelatinosa: Y1 Suppression of Inhibition and Y2 Suppression of Excitation. J. Neurophysiol. *92*, 3266–3275.

Mu, D., Deng, J., Liu, K.-F., Wu, Z.-Y., Shi, Y.-F., Guo, W.-M., Mao, Q.-Q., Liu, X.-J., Li, H., and Sun, Y.-G. (2017). A central neural circuit for itch sensation. Science *357*, 695–699.

Naveilhan, P., Hassani, H., Lucas, G., Blakeman, K.H., Hao, J.-X., Xu, X.-J., Wiesenfeld-Hallin, Z., Thorén, P., and Ernfors, P. (2001). Reduced antinociception and plasma extravasation in mice lacking a neuropeptide Y receptor. Nature *409*, 513–517.

Nichols, M.L., Allen, B.J., Rogers, S.D., Ghilardi, J.R., Honore, P., Luger, N.M., Finke, M.P., Li, J., Lappi, D.A., Simone, D.A., and Mantyh, P.W. (1999). Transmission of chronic nociception by spinal neurons expressing the substance P receptor. Science *286*, 1558–1561.

Padilla, S.L., Qiu, J., Soden, M.E., Sanz, E., Nestor, C.C., Barker, F.D., Quintana, A., Zweifel, L.S., Rønnekleiv, O.K., Kelly, M.J., and Palmiter, R.D. (2016). Agouti-related peptide neural circuits mediate adaptive behaviors in the starved state. Nat. Neurosci. *19*, 734–741.

Papoiu, A.D.P., Coghill, R.C., Kraft, R.A., Wang, H., and Yosipovitch, G. (2012). A tale of two itches. Common features and notable differences in brain activation evoked by cowhage and histamine induced itch. Neuroimage *59*, 3611–3623.

Peirs, C., Williams, S.-P.G., Zhao, X., Walsh, C.E., Gedeon, J.Y., Cagle, N.E., Goldring, A.C., Hioki, H., Liu, Z., Marell, P.S., and Seal, R.P. (2015). Dorsal Horn Circuits for Persistent Mechanical Pain. Neuron *87*, 797–812.

Poindexter, G.S., Bruce, M.A., LeBoulluec, K.L., Monkovic, I., Martin, S.W., Parker, E.M., Iben, L.G., McGovern, R.T., Ortiz, A.A., Stanley, J.A., et al. (2002). Dihydropyridine neuropeptide Y Y(1) receptor antagonists. Bioorg. Med. Chem. Lett. *12*, 379–382.

Ralvenius, W.T., Neumann, E., Pagani, M., Acuña, M.A., Wildner, H., Benke, D., Fischer, N., Rostaher, A., Schwager, S., Detmar, M., et al. (2018). Itch suppression in mice and dogs by modulation of spinal α2 and α3GABA$_A$ receptors. Nat. Commun. *9*, 3230.

Reich, A., Orda, A., Wiśnicka, B., and Szepietowski, J.C. (2007). Plasma neuropeptides and perception of pruritus in psoriasis. Acta Derm. Venereol. *87*, 299–304.

Reich, A., Mędrek, K., Adamski, Z., and Szepietowski, J.C. (2013). Itchy hair–trichoknesis: a variant of trichodynia or a new entity? Acta Derm. Venereol. *93*, 591.

Ringkamp, M., Schepers, R.J., Shimada, S.G., Johanek, L.M., Hartke, T.V., Borzan, J., Shim, B., LaMotte, R.H., and Meyer, R.A. (2011). A role for nociceptive, myelinated nerve fibers in itch sensation. J. Neurosci. *31*, 14841–14849.

Ross, S.E., Mardinly, A.R., McCord, A.E., Zurawski, J., Cohen, S., Jung, C., Hu, L., Mok, S.I., Shah, A., Savner, E.M., et al. (2010). Loss of inhibitory interneurons in the dorsal spinal cord and elevated itch in Bhlhb5 mutant mice. Neuron *65*, 886–898.

Sathyamurthy, A., Johnson, K.R., Matson, K.J.E., Dobrott, C.I., Li, L., Ryba, A.R., Bergman, T.B., Kelly, M.C., Kelley, M.W., and Levine, A.J. (2018). Massively Parallel Single Nucleus Transcriptional Profiling Defines Spinal Cord Neurons and Their Activity during Behavior. Cell Rep. *22*, 2216–2225.

Schmelz, M., Schmidt, R., Bickel, A., Handwerker, H.O., and Torebjörk, H.E. (1997). Specific C-receptors for itch in human skin. J. Neurosci. *17*, 8003–8008.

Schmelz, M., Schmidt, R., Weidner, C., Hilliges, M., Torebjörk, H.E., and Handwerker, H.O. (2003). Chemical response pattern of different classes of C-nociceptors to pruritogens and algogens. J. Neurophysiol. *89*, 2441–2448.

Sciolino, N.R., Plummer, N.W., Chen, Y.-W., Alexander, G.M., Robertson, S.D., Dudek, S.M., McElligott, Z.A., and Jensen, P. (2016). Recombinase-

Dependent Mouse Lines for Chemogenetic Activation of Genetically Defined Cell Types. Cell Rep. *15*, 2563–2573.

Seidler, B., Schmidt, A., Mayr, U., Nakhai, H., Schmid, R.M., Schneider, G., and Saur, D. (2008). A Cre-loxP-based mouse model for conditional somatic gene expression and knockdown in vivo by using avian retroviral vectors. Proc. Natl. Acad. Sci. USA *105*, 10137–10142.

Sieber, M.A., Storm, R., Martinez-de-la-Torre, M., Müller, T., Wende, H., Reuter, K., Vasyutina, E., and Birchmeier, C. (2007). Lbx1 acts as a selector gene in the fate determination of somatosensory and viscerosensory relay neurons in the hindbrain. J. Neurosci. *27*, 4902–4909.

Simone, D.A., Zhang, X., Li, J., Zhang, J.-M., Honda, C.N., LaMotte, R.H., and Giesler, G.J., Jr. (2004). Comparison of responses of primate spinothalamic tract neurons to pruritic and algogenic stimuli. J. Neurophysiol. *91*, 213–222.

Solorzano, C., Villafuerte, D., Meda, K., Cevikbas, F., Bráz, J., Sharif-Naeini, R., Juarez-Salinas, D., Llewellyn-Smith, I.J., Guan, Z., and Basbaum, A.I. (2015). Primary afferent and spinal cord expression of gastrin-releasing peptide: message, protein, and antibody concerns. J. Neurosci. *35*, 648–657.

Solway, B., Bose, S.C., Corder, G., Donahue, R.R., and Taylor, B.K. (2011). Tonic inhibition of chronic pain by neuropeptide Y. Proc. Natl. Acad. Sci. USA *108*, 7224–7229.

Sun, Y.G., and Chen, Z.F. (2007). A gastrin-releasing peptide receptor mediates the itch sensation in the spinal cord. Nature *448*, 700–703.

Sun, Y.G., Zhao, Z.Q., Meng, X.L., Yin, J., Liu, X.Y., and Chen, Z.F. (2009). Cellular basis of itch sensation. Science *325*, 1531–1534.

Szabo, N.E., da Silva, R.V., Sotocinal, S.G., Zeilhofer, H.U., Mogil, J.S., and Kania, A. (2015). Hoxb8 intersection defines a role for Lmx1b in excitatory dorsal horn neuron development, spinofugal connectivity, and nociception. J. Neurosci. *35*, 5233–5246.

Taiwo, O.B., and Taylor, B.K. (2002). Antihyperalgesic effects of intrathecal neuropeptide Y during inflammation are mediated by Y1 receptors. Pain *96*, 353–363.

Taniguchi, H., He, M., Wu, P., Kim, S., Paik, R., Sugino, K., Kvitsiani, D., Fu, Y., Lu, J., Lin, Y., et al. (2011). A resource of Cre driver lines for genetic targeting of GABAergic neurons in cerebral cortex. Neuron *71*, 995–1013.

Todd, A.J., Hughes, D.I., Polgár, E., Nagy, G.G., Mackie, M., Ottersen, O.P., and Maxwell, D.J. (2003). The expression of vesicular glutamate transporters VGLUT1 and VLUGT2 in neurochemically defined axonal populations in the rat spinal cord with emphasis on the dorsal horn. Eur. J. Neurosci. *17*, 13–27.

Wahlgren, C.F., Hägermark, O., and Bergström, R. (1991). Patients' perception of itch induced by histamine, compound 48/80 and wool fibres in atopic dermatitis. Acta Derm. Venereol. *71*, 488–494.

Wang, M., Wang, Q., and Whim, M.D. (2016). Fasting induces a form of autonomic synaptic plasticity that prevents hypoglycemia. Proc. Natl. Acad. Sci. USA *113*, E3029–E3038.

Wende, H., Lechner, S.G., Cheret, C., Bourane, S., Kolanczyk, M.E., Pattyn, A., Reuter, K., Munier, F.L., Carroll, P., Lewin, G.R., and Birchmeier, C. (2012). The transcription factor c-Maf controls touch receptor development and function. Science *335*, 1373–1376.

Wickersham, I.R., Lyon, D.C., Barnard, R.J.O., Mori, T., Finke, S., Conzelmann, K.-K., Young, J.A.T., and Callaway, E.M. (2007). Monosynaptic restriction of transsynaptic tracing from single, genetically targeted neurons. Neuron *53*, 639–647.

Wiley, R.G., and Lappi, D.A. (1999). Targeting neurokinin-1 receptor-expressing neurons with [Sar9,Met(O2)11 substance P-saporin. Neurosci. Lett. *277*, 1–4.

Wu, Y., Wang, C., Sun, H., LeRoith, D., and Yakar, S. (2009). High-efficient FLPo deleter mice in C57BL/6J background. PLoS ONE *4*, e8054.

Zhang, X., Tong, Y.G., Bao, L., and Hökfelt, T. (1999). The neuropeptide Y Y1 receptor is a somatic receptor on dorsal root ganglion neurons and a postsynaptic receptor on somatostatin dorsal horn neurons. Eur. J. Neurosci. *11*, 2211–2225.

STAR★METHODS

KEY RESOURCES TABLE

REAGENT or RESOURCE	SOURCE	IDENTIFIER
Antibodies		
Rabbit α-Calbindin (1:1000)	Swant	Cat# 300; RRID:AB_10000347
Rabbit α-Calretinin (1:1000)	Swant	Cat# 7699/3H; RRID:AB_10000321
Sheep α-CGRP (1:1000)	Abcam	AB22560; RRID:AB_725809
Rabbit α-cMaf (1:5000)	C Birchmeier, MDC, Berlin	N/A
Goat α-cRet (1:250)	R&D Systems	Cat# AF482; RRID:AB_2301030
Goat α-CTb (1:4000),	List Laboratories	Cat# 703; RRID:AB_10013220
Sheep α-Digoxigenin-AP, Fab fragments (1:2000)	Roche	Cat# 11093274910; RRID:AB_514497
Rabbit α-DsRed (1:1000)	Clontech	Cat# 632496; RRID: AB_10013483
Mouse α-Gephyrin (1:8000)	Synaptic Systems	Cat# 147 011; RRID:AB_887717
Rabbit α-GFAP (1:500)	Dako	Cat# Z0334; RRID:AB_10013382
Chicken α-GFP (1:000)	Aves	Cat # GFP-1020; RRID:AB_10000240
Goat α-GFP (1:1000)	Abcam	Cat# ab6673; RRID:AB_305643
Rabbit α-GRPR (1:100)	MBL	Cat# LS-A831; RRID:AB_591750
Rabbit α-GRPR (1:1000)	Abcam	Cat# ab39883; RRID:AB_880315
Guinea pig α-Lmx1b (1:1000)	M Goulding	N/A
Rabbit α-MafA (1:5000)	C Birchmeier, MDC, Berlin	N/A
Mouse α-NeuN (1:1000)	Millipore	Cat# MAB377; RRID:AB_2298772
Rabbit α-Neuropeptide Y1 Receptor (1:100)	Alomone Labs	Cat# ANR-021: RRID:AB_2040030
Rabbit α-NF200 (1:1000)	Sigma	Cat# N4142; RRID:AB_477272
Rabbit α-NK1R (1:500)	Advanced Targeting Systems	Cat# AB-N33ap; RRID:AB_458739
Rabbit α-NPY (1:1000)	Peninsula Lab	Cat# T-4070.0050; RRID:AB_518504
Rabbit α-Pax2 (1:200)	Zymed	Cat# 71-6000; RRID:AB_2533990
Rabbit α-Parvalbumin (1:2000)	Swant	Cat# PV-25; RRID:AB_10000344
Rabbit α-PKCγ (1:1000)	Santa Cruz	Cat# SC-211; RRID:AB_632234
Rat α-RFP (1:1000)	Chromotek	Cat#5F8; RRID: AB_2336064
Goat α-RORα (1:100)	Santa Cruz	Cat# sc-6062; RRID:AB_655755
Rabbit α-S100β (1:500)	Dako	Cat# Z0311; RRID:AB_10013383
Chicken α-TrkB (1:1000)	R&D Systems	Cat# AF1494; RRID:AB_2155264
Goat α-TrkC (1:1000)	R&D Systems	Cat# AF1404; RRID:AB_2155412
Guinea pig α-VGAT (1:1000)	Synaptic Systems	Cat# 131004; RRID:AB_887873
Guinea pig α-vGluT1 (1:1000)	Millipore	Cat# AB5905; RRID: AB_2301751
Bacterial and Virus Strains		
EnvA-pseudotyped, ΔG-mCherry	Janelia Viral Core/HHMI	Wickersham et al., 2007
EnvA-pseudotyped, ΔG-dsRed-Express	Janelia Viral Core/HHMI	Wickersham et al., 2007
AAV2/1-hSyn-DIO-SypHTom	Koch et al., 2017	N/A
Chemicals, Peptides, and Recombinant Proteins		
Isolectin GS-IB4 From Griffonia simplicifolia, Alexa Fluor 647 Conjugate (1:500)	Invitrogen	Cat# I32450; RRID:SCR_014365
Cholera Toxin Subunit b (Recombinant), Alexa Fluor 647 Conjugate	Invitrogen	Cat# C34778
Diphtheria Toxin, Unnicked, from Corynebacterium diphtheria	List Laboratories	Cat# 150
Clozapine *N*-oxide	Sigma	Cat# C0832
Blank saporin	Advanced Targeting Systems	Cat# IT-21

(*Continued on next page*)

Continued

REAGENT or RESOURCE	SOURCE	IDENTIFIER
Bombesin-saporin	Advanced Targeting Systems	Cat# IT-40
[Sar^9, $Met(O_2)^{11}$]-substance P-saporin	Advanced Targeting Systems	Cat# IT-11
Neuropeptide Y (human, rat)	Tocris	Cat# 1153
[Leu^{31}, Pro^{34}]-NPY (100 μg kg^{-1})	M Goulding	N/A
BIBP 3226 trifluoroacetate	Tocris	Cat# 2707/1
BMS 193885	Tocris	Cat# 3242/10
Chloroquine diphosphate	Sigma	Cat# C6628
Histamine	Sigma	Cat# H7125
Compound 48/40	Sigma	Cat# C2313
SLIGRL-NH_2	Abcam	Cat# ab120176
Capsaicin	Sigma	Cat# M2028
Formalin	Sigma	Cat# HT501128
Kynurenic acid	Sigma	Cat# K3375
Picrotoxin	Sigma	Cat# P1675
Strychnine	Sigma	Cat# S0532
NBT	Roche	Cat# 11383213001
BCIP	Roche	Cat# 11383221001
Experimental Models: Organisms/Strains		
Mouse: *$Y1^{Cre}$*	The Jackson Laboratory	JAX stock #030544; RRID:IMSR_JAX:030544
Mouse: *FLPo-10*	The Jackson Laboratory	JAX stock #011065; RRID:IMSR_JAX:011065
Mouse: *Y1::eGFP*	Gene Expression Nervous System Atlas (GENSAT)	RRID:MMRRC_010554-UCD
Mouse: *NPY::Cre*	Bourane et al., 2015a	N/A
Mouse: *Sst^{Cre}*	The Jackson Laboratory	JAX stock #013044; RRID:IMSR_JAX:013044
Mouse: *Sst^{FlpO}*	The Jackson Laboratory	JAX stock #028579; RRID:IMSR_JAX:028579
Mouse: *$Lbx1^{Cre}$*	Sieber et al., 2007	MGI: 104867
Mouse: *$Lbx1^{FlpO}$*	Bourane et al., 2015a	N/A
Mouse: *$Ai14^{lsl\text{-}Tom}$*	The Jackson Laboratory	JAX stock #007908; RRID:IMSR_JAX:007908
Mouse: *$Ai65^{ds\text{-}Tom}$*	The Jackson Laboratory	JAX stock #021875; RRID:IMSR_JAX:021875
Mouse: *$R26^{ds\text{-}hM3D}$*	The Jackson Laboratory	JAX stock #026942; RRID:IMSR_JAX:026942
Mouse: *$R26^{ds\text{-}hM4D}$*	Bourane et al., 2015a	N/A
Mouse: *$R26^{ds\text{-}HTB}$*	Bourane et al., 2015b	N/A
Mouse: *$R26^{ds\text{-}ReaChR}$*	Hooks et al., 2015	JAX stock #024846; RRID:IMSR_JAX:024846
Mouse: *$R26^{lsl\text{-}TVA}$*	Seidler et al., 2008	MGI:3814188
Mouse: *$Tau^{ds\text{-}DTR}$*	Britz et al., 2015	N/A
Mouse: *NPY KO*	Karl et al., 2008	N/A
Mouse: *$Y1^{f/f}$*	Bertocchi et al., 2011	N/A
Mouse: GRP::eGFP	MMRRC	RRID:MMRRC_010444-UCD
Software and Algorithms		
Adobe Illustrator and Photoshop CS5	Adobe	https://www.adobe.com
Prism 5	GraphPad	https://www.graphpad.com
Excel 365	Microsoft	https://www.microsoft.com/en-us/
ImageJ Cell Counter Plugin	Kurt de Vos, Univ. of Sheffield, UK	https://imagej.nih.gov/ij
pClamp10.4 and Clampfit	Molecular Devices	https://www.moleculardevices.com

LEAD CONTACT AND MATERIALS AVAILABILITY

Further information and requests for resources and reagents should be directed to and will be fulfilled by the Lead Contact, Martyn Goulding (goulding@salk.edu).

EXPERIMENTAL MODEL AND SUBJECT DETAILS

All protocols for animal experiments were approved by the IACUC of the Salk Institute for Biological Studies according to NIH guidelines for animal experimentation. Male and female mice were used in all studies. Animals were randomized to experimental groups and no sex differences were noted.

The *Y1^{Cre}* knockin mouse line was generated by Padilla et al. (Padilla et al., 2016). An FRT-flanked neomycin cassette was removed by crossing with the *FLPo-10* deleter strain (Wu et al., 2009), as described by Padilla et al. (Padilla et al., 2016). The *Y1::eGFP* transgenic reporter mouse line (RRID:MMRRC_010554-UCD) was generated by the Gene Expression Nervous System Atlas (GENSAT) project. The following mouse lines were also used in this study: *NPY::Cre* (Bourane et al., 2015a), *Sst^{Cre}* (Taniguchi et al., 2011), *Sst^{FlpO}* (He et al., 2016), *Lbx1^{Cre}* (Sieber et al., 2007), *Lbx1^{FlpO}* (Bourane et al., 2015a), *Ai14$^{lsl\text{-}Tom}$* (Madisen et al., 2010), *Ai65$^{ds\text{-}Tom}$* (Madisen et al., 2015), *R26$^{ds\text{-}hM3D}$* (Sciolino et al., 2016), *R26$^{ds\text{-}hM4D}$* (Bourane et al., 2015a), *R26$^{ds\text{-}ReaChR}$* (Hooks et al., 2015), *Tau$^{ds\text{-}DTR}$* (Britz et al., 2015), *NPY KO* (Karl et al., 2008), *Y1$^{f/f}$* (Bertocchi et al., 2011), *GRP::eGFP* (Mishra and Hoon, 2013), *R26$^{ds\text{-}HTB}$* (Bourane et al., 2015b), *R26$^{lsl\text{-}TVA}$* (Seidler et al., 2008).

METHOD DETAILS

Immunohistochemistry

Mice were euthanized by a single intraperitoneal (i.p.) injection (10 μl g^{-1} body weight) of ketamine (10 mg ml^{-1}) and xylazine (1 mg ml^{-1}) immediately prior to perfusion with 20 mL ice-cold 4% paraformaldehyde in PBS. Spinal cords and DRG (lumbar levels L_4 and L_5) were dissected and post-fixed for 1 h at RT, then washed 3 times in PBS and cryoprotected in 30% sucrose-PBS (w/v) overnight at 4°C. Tissue was embedded in Tissue-Tek OCT Compound (Sakura Finetek) and cryosectioned at 40 μm. Sections were dried at RT and stored at −20°C. Sections were washed once with PBS (5 min), blocked with a solution of 10% donkey serum in PBT (PBS, 0.1% Triton X-100) for 1 h at RT and then incubated overnight at 4°C with primary antibodies in a solution of 1% donkey serum in PBT. Sections were then washed 3 times (15 min each) in PBT before being incubated for 2 h at RT with fluorophore–conjugated secondary antibodies (1:1000; Jackson Laboratories) in a solution of 1% donkey serum in PBT. Sections were again washed 3 times (15 min each) in PBT before being mounted with Aqua-Poly/Mount (Polysciences). A Zeiss LSM 700 confocal microscope was used to capture images. 3-5 spinal cords were analyzed for each condition. ImageJ software was used to assess immunofluorescence, with thresholds set according to signal intensity (Jensen, 2013).

The following primary antibodies were used in this study: rabbit α-Calbindin (1:1,000; Swant), rabbit α-Calretinin (1:1,000; Swant), sheep α-CGRP (1:1,000; Abcam), rabbit α-cMaf (1:5000; C Birchmeier, MDC, Berlin), goat α-cRet (1:250; R&D Systems), goat α-CTB (1:4000; List Laboratories), rabbit α-DsRed (1:1000; Clontech), mouse α-Gephyrin (1:8000; Synaptic systems); rabbit α-GFAP (1:500; Dako), chicken α-GFP (1:000; Aves), goat α-GFP (1:1000; Abcam), rabbit α-GRPR (1:1000; Abcam), rabbit α-GRPR (1:100; MBL), guinea pig α-Lmx1b (1:1000; M Goulding), mouse α-NeuN (1:1000; Millipore), rabbit α-NK1R (1:500; Advanced Targeting Systems), rabbit α-NPY (1:1000; Peninsula Lab), rabbit α-Parvalbumin (1:1000; Swant), rabbit α-Pax2 (1:200; Zymed), rat α-RFP (1:1000; Chromotek), rabbit α-PKCγ (1:1000; Santa Cruz), goat α-RORα (1:100; Santa Cruz), rabbit α-S100β (1:500; Dako), goat TrkB (1:1000; R&D Systems), goat α-TrkC (1:1000; R&D Systems), guinea pig α-VGAT (1:1000; Synaptic Systems), guinea pig α-vGluT1 (1:1000; Millipore). In addition, Alexa Fluor 647-conjugated isolectin GS-IB4 from *Griffonia simplicifolia* (Invitrogen) was used at 1:500.

In Situ Hybridization

For *in situ* hybridization (ISH), mice were perfused with 4% paraformaldehyde in a solution of 0.1% diethyl pyrocarbonate in PBS (PBS-DEPC), post fixed for 1 h at RT, washed 3 times with PBS-DEPC and cryopreserved overnight in 30% sucrose in PBS-DEPC. Spinal cords were embedded in Tissue-Tek and stored at −80°C. Spinal cords were then cryosectioned at 16 μm, and sections were hybridized with an antisense RNA probe overnight at 64°C. Sections were washed twice in a solution of 1 x saline-sodium citrate buffer, 50% formamide, and 0.1% Tween-20 at 64°C for 30 min and blocked with a solution of 0.1% Tween 20 in maleic acid buffer (MABT) containing 2% blocking reagent and 10% inactivated sheep serum for 2 h at RT. Sections were then incubated overnight with sheep α-digoxigenin-alkaline-phosphatase Fab fragments (1:2000; Roche), washed twice in MABT and revealed with a staining solution of NBT (1:500, Roche) and BCIP (1:600, Roche). An Olympus VS-120 Virtual Slde Scanning Microscope was used for imaging. For double staining analyses, tdTomato fluorescence was imaged before ISH was performed. ISH images were later pseudo-colored and superposed onto the tdTomato signal in Photoshop (Adobe Systems). For quantification, three sections from each of three spinal cords were analyzed per condition, and only cells with clearly visible nuclei were scored.

Rabies Virus Tracing and Morphological Analyses

For the sparse labeling of *Y1^{Cre}* neurons required for morphological reconstruction, EnvA-pseudotyped, ΔG-dsRed-Express rabies virus (100 μl, 1.28 × 10^8 units ml^{-1}) was injected unilaterally into the lumbar spinal cord of P10 *Y1^{Cre}; R26$^{lsl\text{-}TVA}$* mice (Bourane et al., 2015b). For the transsynaptic tracing studies, bilateral injections of EnvA-pseudotyped, ΔG-mCherry (250 μl, 3.3 × 10^{10} units ml^{-1}) were made into the lumbar cord of *Y1^{Cre}; Lbx1^{FlpO}; R26$^{ds\text{-}HTB}$* animals at P5.

Briefly, mice were anesthetized by administering 2.5% isoflurane via a nose cone. The skin over the lumbar region of the dorsal spinal cord was incised and a laminectomy was performed at the T_{13}-L_1 level. After removal of the dura mater with a fine needle

to expose the spinal cord, virus was injected via a fine glass capillary inserted into the dorsal spinal cord. The needle was left in the cord for 1 min after injection to prevent outflow. The skin was closed using Vetbond (3M) and Reflex Skin Closure System (CellPoint Scientific). Mice were perfused 5 days post-injection and processed for immunohistochemistry.

AAV Virus Tracing of Synaptic Connections

To visualize synaptophysin at presynaptic boutons, injections of AAV2/1-hSyn-DIO-SypHTomato (0.5 μl, 1.6×10^{12} units ml^{-1}) were made into the lumbar spinal cord of P37 *Y1::eGFP* mice as described above. Spinal cords were then processed for immunohistochemistry at P60.

Retrograde Cholera Toxin-b Labeling of Cutaneous Sensory Neurons

Postnatal day (P) 39 *Y1Cre; Ai14$^{lsl\text{-}Tom}$* mice were anesthetized with 2.5% isoflurane in O2, and Alexa Fluor 647-conjugated cholera toxin subunit B (CTb) (0.5 μl, 2.5 μg μl^{-1} in 0.9% sterile saline; Molecular Probes) was injected into either the hairy skin of the hindlimb or the glabrous skin of the plantar hindpaw with a fine glass capillary. Mice were perfused at 3 days post injection and processed for immunohistochemistry.

Cell Ablation

For ablation of neurons expressing Cre and FlpO drivers in addition to *Tau$^{ds\text{-}DTR}$*, mice were injected with diphtheria toxin (DT; 50 ng kg^{-1} in 0.9% sterile saline, i.p.; List Biological Laboratories) at P28 and P31 (Bourane et al., 2015a). Analysis of spontaneous scratching in mice expressing *NPY::Cre* (and relevant controls) was performed at P35, 7 days following the first DT injection. For the double-Cre ablation experiment, controls were positive for Cre and *Tau$^{ds\text{-}DTR}$* alleles but lacked the *Lbx1^{FlpO}* allele and did not therefore express the diphtheria toxin receptor; however, all mice received DT. All other behavioral testing was performed 14-21 days following the first injection; controls were littermates of experimental animals and had identical genotypes but received injections of 0.9% sterile saline instead of DT.

To ablate cells cell populations with saporin-conjugated receptor ligands, P28 mice were given a single intrathecal (i.t.) injection of either bombesin-saporin (400 ng in 5 μL 0.9% sterile saline; Advanced Targeting Systems) (Bourane et al., 2015a) to ablate $GRPR^+$ cells or [Sar^9, $Met(O_2)^{11}$]-substance P-saporin neurons (100 ng in 5 μL 0.9% sterile saline; Advanced Targeting Systems) to ablate $NK1R^+$ neurons (Wiley and Lappi, 1999). Littermate controls received blank saporin (equal mass in 5 μL 0.9% sterile saline; Advanced Targeting Systems). Behavioral testing and assessment of ablation efficiency by immunohistochemistry were performed 14 days later at P42.

For i.t. injections, mice were anesthetized with 2.5% isoflurane in O_2, delivered via a nose cone. The caudal paralumbar region was then secured between the thumb and index finger, and a 30-gauge needle was inserted into the fifth intervertebral space until it elicited a tail flick. To prevent outflow, the needle was held in place for 10 s and turned 90° prior to withdrawal.

Drug Administration

Synthesis of the selective Y1 receptor agonist [Leu^{31}, Pro^{34}]-Neuropeptide Y ([Leu^{31}, Pro^{34}]-NPY; YPSKPDNPGEDAPAEDMARYYS ALRHYINLLTRPRY-NH_2) (Fuhlendorff et al., 1990) was performed on a Gyros Protein Technologies, Inc. Tribute peptide synthesizer equipped with real-time UV monitoring, using standard Fmoc chemistry, in the Salk's Peptide Synthesis Core. The resultant crude peptide was purified by the Salk's Proteomics Core to > 98% using HPLC. The final, purified product gave a single peak of predicted mass (4240.7 Da) by MS analysis. The peptide was administered in solution at pH 7.

Neuropeptide Y (NPY; Tocris) and [Leu^{31}, Pro^{34}]-NPY were dissolved in 0.9% sterile saline. Clozapine *N*-oxide (CNO; Sigma) and the Y1 receptor antagonist BIBP 3226 (Tocris) (Jacques et al., 1995) were dissolved in DMSO, which was then diluted with 0.9% sterile saline such that the concentration of DMSO did not exceed 1% in injected solutions. The Y1 receptor antagonist BMS 193885 (Tocris) (Poindexter et al., 2002) was dissolved in sterile water, which was then rendered isotonic with glucose (5% w/v).

CNO was administered by i.p. injection at 2 mg kg^{-1}. Other drugs were administered as indicated.

CNO, NPY, [Leu^{31}, Pro^{34}]-NPY, and BIBP 3226 were injected 15 min prior to behavioral testing. BMS 193885 was observed to cause inactivity for ~30 min following i.p. injection, as previously reported (Antal-Zimanyi et al., 2008); behavioral testing in BMS 193885-injected mice and vehicle-injected controls was therefore conducted from 30 to 60 min post injection. WT mice injected with NPY, [Leu^{31}, Pro^{34}]-NPY, BIBP 3226 or BMS 193885 were compared to vehicle-injected littermate controls.

To take into account differences in phenotype severity between *NPY::Cre; Lbx1^{FlpO}; Tau$^{ds\text{-}DTR}$* mice treated with DT and between *Lbx1^{Cre}; Y1$^{f/f}$* mice, paired t tests were conducted to assess the effects of Y1 drugs. Recordings were made at 4 h intervals on the same day.

For chemogenetic silencing and activation experiments, all mice received CNO. Control mice were positive for the Cre and *R26$^{ds\text{-}hM4D}$* or *R26$^{ds\text{-}hM3D}$* alleles but lacked the *Lbx1^{FlpO}* allele and did not therefore express the hM4D or hM3D receptor.

Electrophysiology

For slice preparations, P14-28 mice were anaesthetized by i.p. injection of urethane (10 μl/g) and transcardially perfused with oxygenated ice-cold dissecting/recovery artificial cerebrospinal fluid (ACSF; NaCl, 95 mM; KCl, 2.5 mM; $NaHCO_3$, 26 mM; $NaH_2PO_4H_2O$, 1.25 mM; $MgCl_2$, 6 mM; $CaCl_2$, 1.5mM; glucose, 20 mM; sucrose, 50 mM; Kynurenic Acid, 1 mM; ethyl pyruvate, 5 mM). The spinal

cords were then isolated in ice-cold dissecting/recovery ACSF before being embedded in low-melting agarose at 33°C. A vibratome (Leica VT1000S) was used to cut 300 μm transverse slices from lumbar segments L_1-$_5$ in ice cold dissecting/recovery ACSF. Slices were then allowed to recover in dissecting/recovery ACSF at ~34°C for 1 h before being secured in a recording chamber continuously perfused with recording aCSF (NaCl, 125 mM; KCl, 2.5 mM; $NaHCO_3$, 26 mM; $NaH_2PO_4H_2O$, 1.25 mM; $MgCl_2$, 1 mM; $CaCl_2$, 2 mM; glucose, 20 mM; ethyl pyruvate, 5 mM) at RT. At all stages, ACSF was equilibrated with carbogen (95% O_2; 5% CO_2). Experiments were performed at RT.

Patch-clamp electrodes (3–5 MΩ) were pulled on a horizontal puller (Sutter Instrument, Novato, CA) from borosilicate glass (World Precision Instruments, Sarasota, FL). Signals were amplified and filtered (4 kHz low-pass Bessel filter) with a MultiClamp 700B amplifier (Molecular Devices) and acquired at 50 kHz with a Digidata 1440A A/D board and pCLAMP software (Molecular Devices). Neuronal firing was elicited by injecting depolarizing currents ranging from 0 to 200 pA in 20 pA increments for 1 s at intervals of 10 s. For ReaChR-mediated stimulation of NPY::Cre INs, a single LED optic fiber source (~2 mW output at 591 nm) was positioned ~10 mm from the surface of the slice, illuminating its entire surface. Stimulation was delivered at a pulse width of 5-20 ms. All drugs were bath applied. Kynurenic acid (1.5 mM; Sigma) and strychnine (1 μM; Sigma) were dissolved in water. Picrotoxin (60 μM; Sigma) was dissolved in DMSO such that the concentration of DMSO in recording solution did not exceed 0.1% (v/v). A liquid junction potential of 14 mV was corrected offline.

Behavioral Testing

Littermate controls were used for behavioral tests, and the experimenter was blinded to genotype/treatment. Animals were habituated to the behavioral testing apparatus for 1 h on each of the two days preceding data collection. Tests were conducted at P42-P49, or at P35 (7 days following the first injection of DT) in experiments to assess spontaneous scratching induced by ablation of *NPY::Cre* neurons.

Spontaneous Itch

To quantify scratching induced in the absence of an experimental mechanical stimulus (spontaneous itch), mice were placed in a plastic chamber and video recorded for a period of 30 min; bouts of hindlimb scratching were counted offline (Bourane et al., 2015a).

Nape Stimulation Assay

To quantify itch-related scratching behaviors induced by mechanical stimulation of the hairy skin, mice were placed in a plastic chamber and a 0.16 g von Frey hair was applied to the nape for 3 s (as per Bourane et al., 2015a). Hindlimb scratching responses over 10 trials were counted and reported as a percentage.

von Frey Assay

To assess the sensitivity of the glabrous skin to light punctate mechanical stimulation, mice were placed in a plastic chamber on an elevated wire grid and the lateral plantar surface of the hindpaw was stimulated with calibrated von Frey monofilaments (0.008-4 g). The paw withdrawal threshold for the von Frey assay was determined by Dixon's up-down method (Chaplan et al., 1994).

Dynamic Touch Test

To assess the sensitivity of the glabrous skin to light dynamic touch, mice were placed in a plastic chamber on an elevated wire grid and the plantar surface of the hindpaw was stimulated by light stroking with a fine paintbrush in a heel-to-toe direction (Bourane et al., 2015b). The test was repeated 10 times at 10 s intervals between trails, and the percentage of positive paw withdrawal trials was calculated.

Pinprick Test

To assess the sensitivity of the glabrous skin to acute painful stimuli, mice were placed in a plastic chamber on an elevated wire grid and the plantar surface of the hindpaw was stimulated with an Austerlitz insect pin (Tip diameter: 0.02 mm; Fine Science Tools). The pin was gently applied to the plantar surface of the hindpaw without moving the paw or penetrating the skin. The pin stimulation was repeated 10 times on different paw areas with a 1-2 min interval between trails, and the percentage of trials in which mice responded with paw withdrawal was calculated.

Randall-Selitto Test

Prior to testing, mice were placed in a plastic restraining tube and allowed 5 min to acclimatize. A Randall-Selitto device (IITC, USA) was used to apply slowly increasing pressure to a point midway along the tail until the animal showed clear signs of discomfort. This pressure was recorded as the pain threshold. Three trials taken at 2 min intervals were performed to calculate the average threshold for each animal.

Chemical Nociception Tests

To assess pain induced by chemical agents, a 30-gauge needle was used to inject 6 mL of either capsaicin (1 mg in 10 mL 9% saline containing 7% Tween-80) or formalin (2% in 9% saline) subcutaneously into the plantar hindpaw. The time spent licking, flinching, and biting the injected hindpaw was recorded for 15 min (capsaicin) or 1 h (formalin) post-injection. Phase I was defined as the first 10 min post injection and phase II was defined as the period 10-60 min post injection.

Hot Plate Test

Mice were placed on a hot plate (IITC, USA) set at 46°C, 50°C or 54°C and the latencies to hindpaw flinching and licking were measured. All animals were tested sequentially with a minimum of 5 min between each test. To prevent tissue damage, a cutoff time was set at 60 s for assays at 46°C and 50°C, and 30 s for 54°C.

Hargreaves Test

To measure radiant heat pain, mice were placed in a plastic chamber and the plantar hindpaw surface was exposed to a beam of radiant heat (IITC, USA). The latency to paw withdrawal was determined in one trial per hindpaw and averaged per animal, with a 10 min interval between trials. A cutoff time of 30 s was set to prevent tissue damage.

Chemical Itch Test

The pruritogens chloroquine (200 μg; Sigma), histamine (100 μg; Sigma), compound 48/80 (100 μg; Sigma) and SLIGRL-NH_2 (SLIGRL; 100 nM; Abcam) were dissolved in 0.9% sterile saline and injected intradermally behind the ear in a volume of 50 μl. The behavior of each animal was video-recorded over the following 30 min, and the number of hindpaw scratch bouts was counted.

QUANTIFICATION AND STATISTICAL ANALYSIS

Data were analyzed in GraphPad Prism 6 for Windows, Version 6.01 (Graphpad Software) or Excel 2016 (Microsoft) by two-tailed, unpaired t tests, unless otherwise indicated. See figure legends for details of statistical analyses. $p < 0.05$ was considered to be statistically significant. All data are presented as the mean ± standard error of the mean (SEM).

All tdTomato signals were enhanced by RFP antibody staining prior to analysis.

Cell Reports, Volume *28*

Supplemental Information

Spinal Neuropeptide Y1 Receptor-Expressing Neurons Form an Essential Excitatory Pathway for Mechanical Itch

David Acton, Xiangyu Ren, Stefania Di Costanzo, Antoine Dalet, Steeve Bourane, Ilaria Bertocchi, Carola Eva, and Martyn Goulding

Supplemental Information

Spinal NPY1R+ Neurons form an Essential Excitatory Pathway for Mechanical Itch

David Acton, Xiangyu Ren, Stefania Di Costanzo, Antoine Dalet, Steeve Bourane, Illarai Bertocchi, Carola Eva, and Martyn Goulding

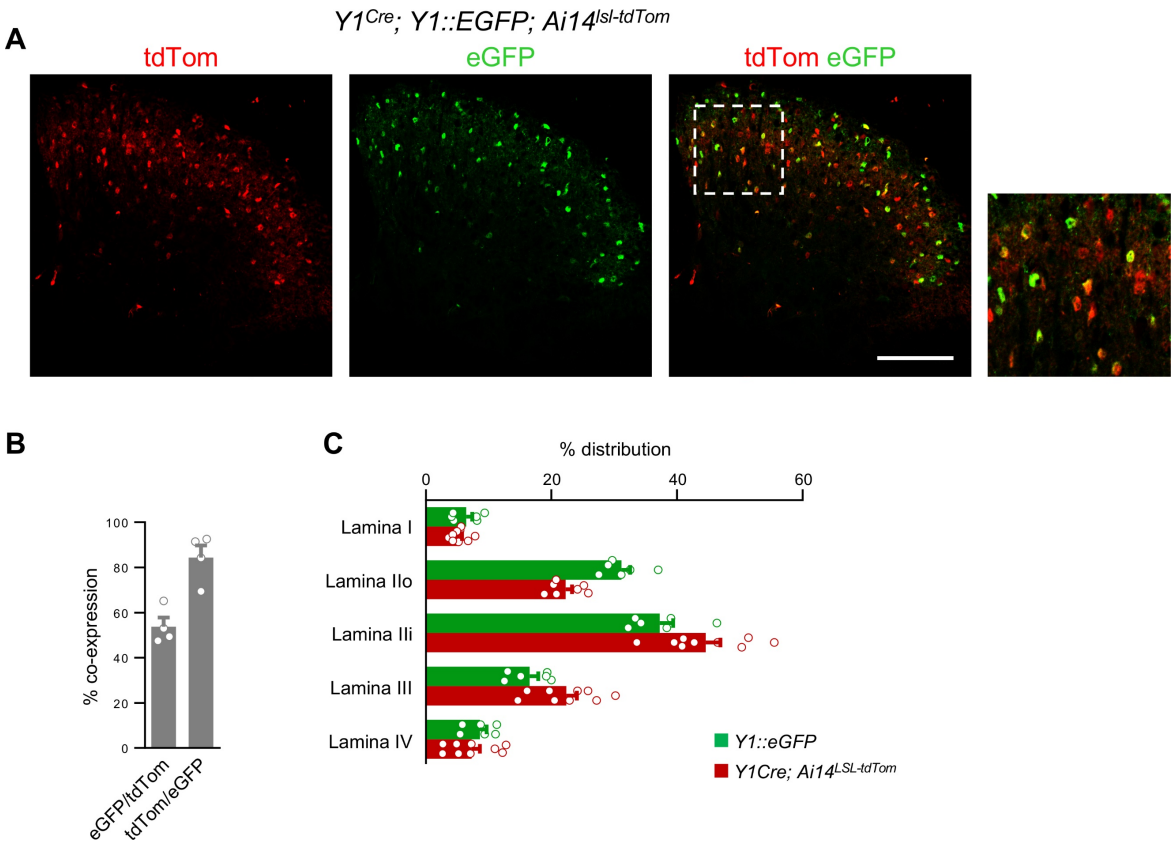

Figure S1 related to Figure 1. Characterization of *Y1::EGFP* expression.

(A) Sections from the lumbar spinal cord of a P42 *Y1^{Cre}; Y1::EGFP; Ai14$^{lsl\text{-}tdTom}$* mouse showing overlapping expression of tdTomato and eGFP. Scale bar: 100 µm. **(B)** Summary of tdTomato and eGFP co-expression (n = 4 mice). **(C)** Comparison of Y1-tdTomato and Y1-eGFP expression by lamina (n = 6-9 mice). Data: mean ± SEM.

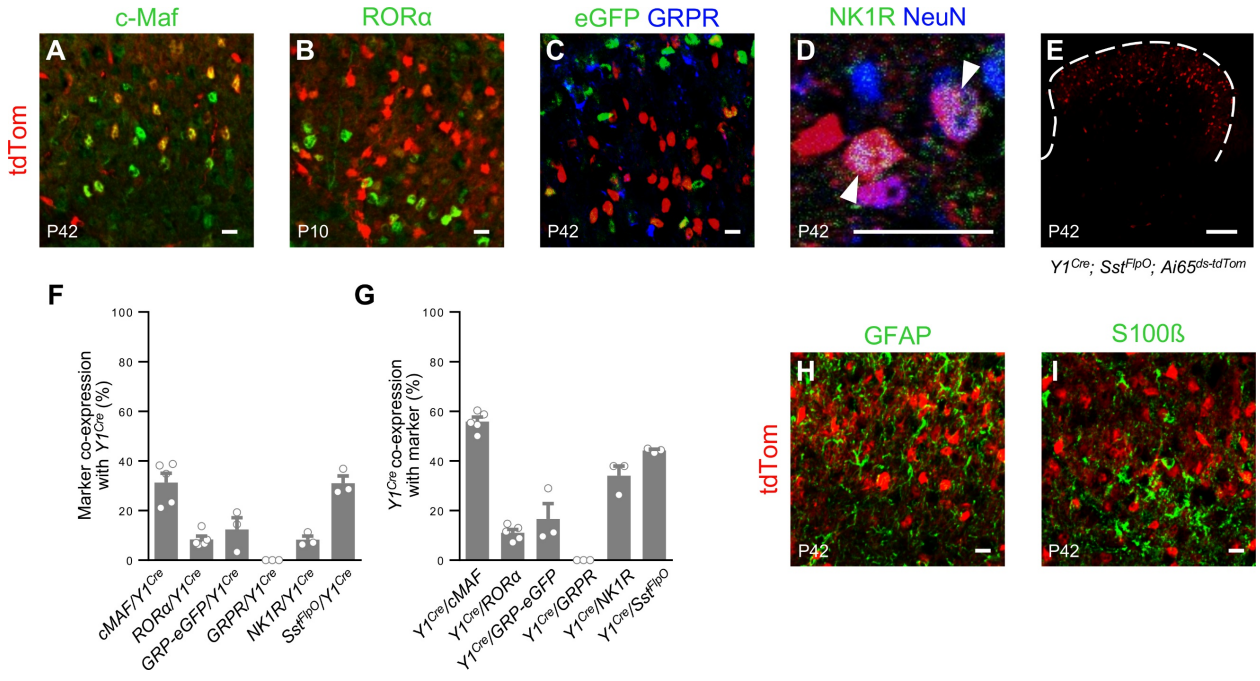

Figure S2 related to Figure 1. Co-expression of markers of dorsal horn cell populations with *Y1^{Cre}*.

(A-D) Sections of lumbar spinal cords showing co-expression of *Y1^{Cre}* with markers of dorsal horn excitatory neurons: cMaf co-expression was assessed by antibody staining in lumbar spinal cord sections from P42 *Y1^{Cre}; Ai14$^{lsl\text{-}tdTom}$* mice (A). RAR-related orphan receptor alpha (RORα) expression was assessed by antibody labelling in P10 *Y1^{Cre}; Ai14$^{lsl\text{-}tdTom}$* mice (B). Co-expression of *Y1^{Cre}* with gastrin releasing peptide (GRP) and antibody-labeled gastrin-releasing peptide receptor (GRPR) was assessed in P42 *Y1^{Cre}; Ai14$^{lsl\text{-}tdTom}$; GRP::eGFP* mice (C). Neurokinin-1 receptor (NK1R) co-expression was assessed by antibody staining in lumbar spinal cord sections from P42 *Y1^{Cre}; Ai14$^{lsl\text{-}tdTom}$* mice; an antibody against the pan-neuronal marker NeuN was employed to facilitate identification of Y1-tdTomato^{-} cells. Arrowheads: Y1-tdTomato^{-}/NK1R^{+} neurons (D). **(E)** Somatostatin (Sst) co-expression was assessed by comparing Y1^{+}/Sst^{+} neurons in P42 *Y1^{Cre}; Sst^{FlpO}; Ai65$^{ds\text{-}tdTom}$* mice. **(F and G)** Quantification of the data exemplified in panels A-E: the proportions of Y1^{Cre} neurons co-expressing markers of other neuronal populations (F) and of those other populations co-expressing tdTomato (G). **(H and I)** tdTomato did not colocalize with antibody-labeled GFAP (H) or S100ß (I), markers of glia. *n* = 3-5 mice for each condition. Scale bars: 100 µm. Data: mean ± SEM.

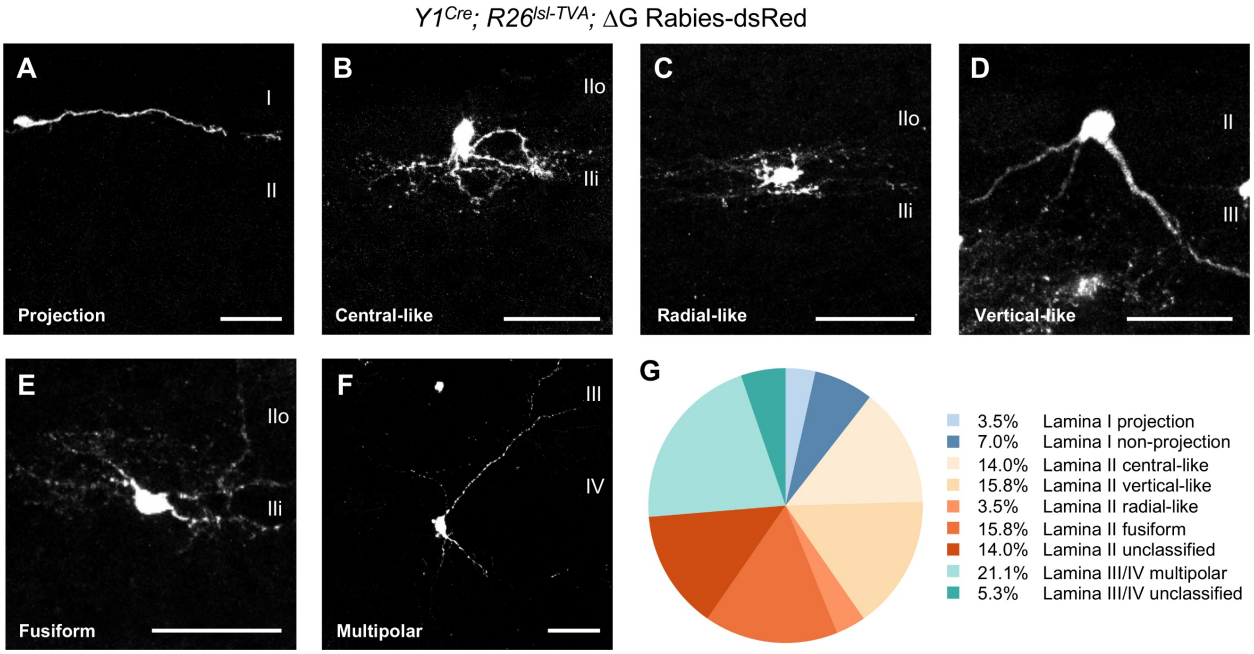

Figure S3 related to Figure 1. Morphological analysis of *Y1*^{Cre} neurons.

(A-F) Examples of laminae I-IV Y1^{Cre} neuron morphologies (red) in sagittal sections from the lumbar spinal cord of P15 *Y1*^{Cre}*; R26*$^{lsl\text{-}TVA}$ mice injected with EnvA ΔG dsRed-rabies virus at P10. **(G)** Quantification of Y1^{Cre} neuronal morphologies in laminae I-IV. n = 53 cells from 5 mice. Scale Bars: 50 µm.

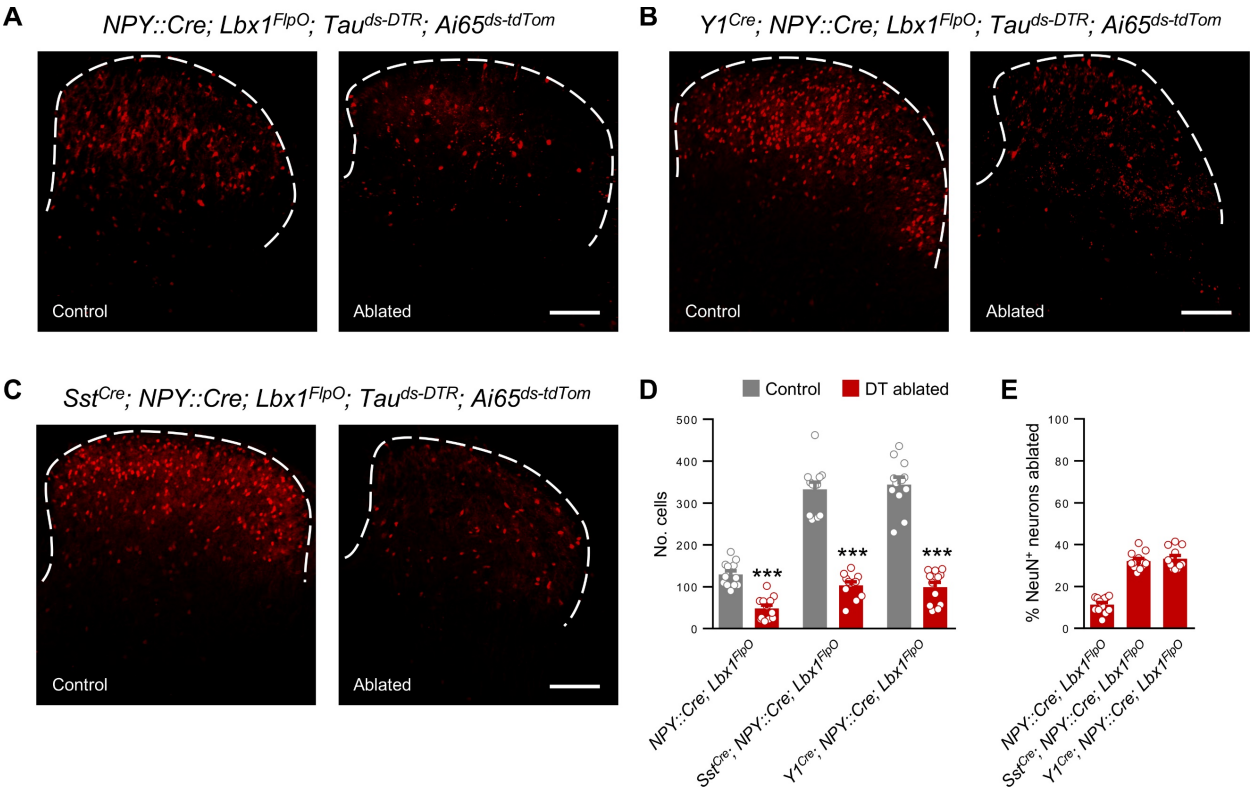

Figure S4 related to Figure 3. Ablation efficiency in NPY::Cre IN phenotype-recovery experiment.

(**A-C**) Transverse sections through the lumbar spinal cords of P49 mice treated with saline (control, left) or DT (ablated, right): *NPY::Cre; Lbx1^{FlpO}; Tau$^{ds\text{-}DTR}$; Ai65$^{ds\text{-}tdTom}$* (A), *Y1^{Cre}; NPY::Cre; Lbx1^{FlpO}; Tau$^{ds\text{-}DTR}$; Ai65$^{ds\text{-}tdTom}$* (B), *Sst^{Cre}; NPY::Cre; Lbx1^{FlpO}; Tau$^{ds\text{-}DTR}$; Ai65$^{ds\text{-}tdTom}$* (C). **(D)** Summary of cell numbers for each condition. The ablation efficiency, assessed as percentage reduction in cell number, did not differ between genotypes (one-way ANOVA, $p > 0.5$). **(E)** Percentage reduction of NeuN$^+$ neurons in laminae I-IV for each DT-treated phenotype. $n = 3$ sections from 4 mice per condition. Scale bars: 100 µm. ***$p < 0.001$. Data: mean ± SEM.

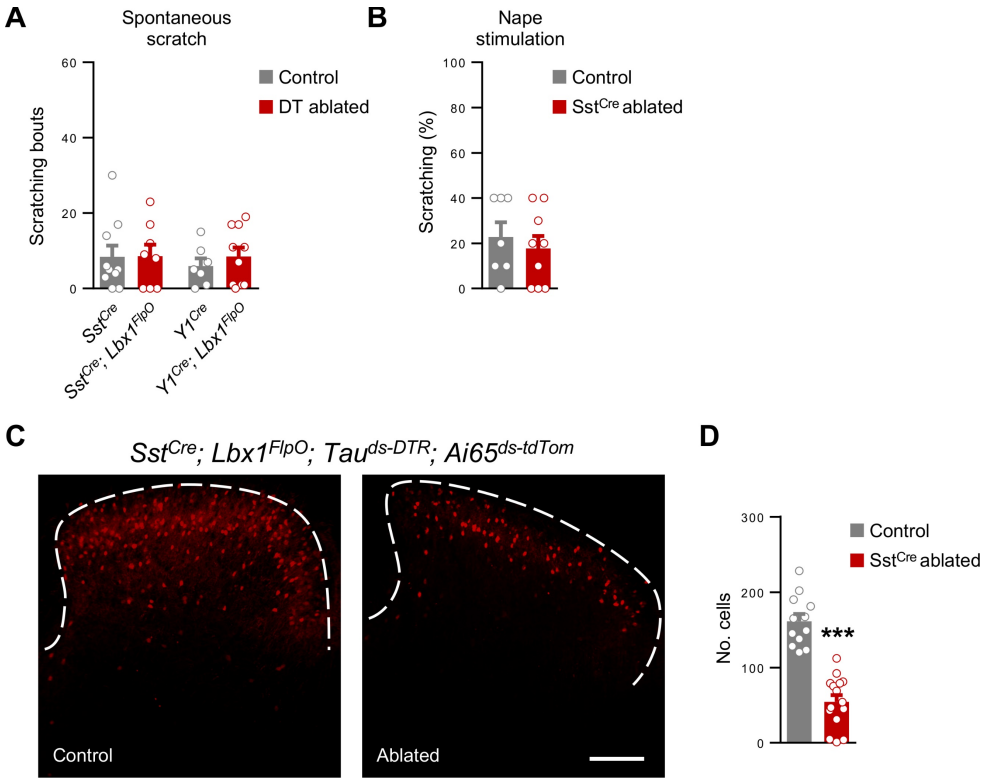

Figure S5 related to Figure 3. Sst^{Cre} neurons do not determine sensitivity to mechanical itch.

(A) Spontaneous scratching is unchanged in mice 1 week after ablation of dorsal horn Sst^{Cre} (*Sst^{Cre}; Lbx1^{FlpO}; Tau^{ds-DTR}; Ai65$^{ds-tdTom}$*; $n = 8$) or Y1^{Cre} neurons (*Y1^{Cre}; Lbx1^{FlpO}; Tau^{ds-DTR}; Ai65$^{ds-tdTom}$*, $n = 10$) compared with DT-treated controls lacking FlpO-dependent DT-receptor expression (*Sst^{Cre}; Tau^{ds-DTR}; Ai65$^{ds-tdTom}$*, $n = 10$; *Y1^{Cre}; Tau^{ds-DTR}; Ai65$^{ds-tdTom}$*, $n = 7$). **(B)** Scratching responses to stimulation of the nape by a 0.16 g von Frey hair are unchanged when Sst^{+} neurons are ablated in *Sst^{Cre}; Lbx1^{FlpO}; Tau^{ds-DTR}; Ai65$^{ds-tdTom}$* mice treated with DT ($n = 9$) compared with saline-treated controls ($n = 7$). **(C)** Sections of lumbar spinal cords from P49 *Sst^{Cre}; Lbx1^{FlpO}; Tau^{ds-DTR}; Ai65$^{ds-tdTom}$* mice treated with saline (control) or DT (ablated). **(D)** Summary of ablation efficiency (control, $n = 4$ mice; ablated, $n = 5$; 3 sections per cord). Scale bars: 100 µm. ***$p < 0.001$. Data: mean ± SEM.

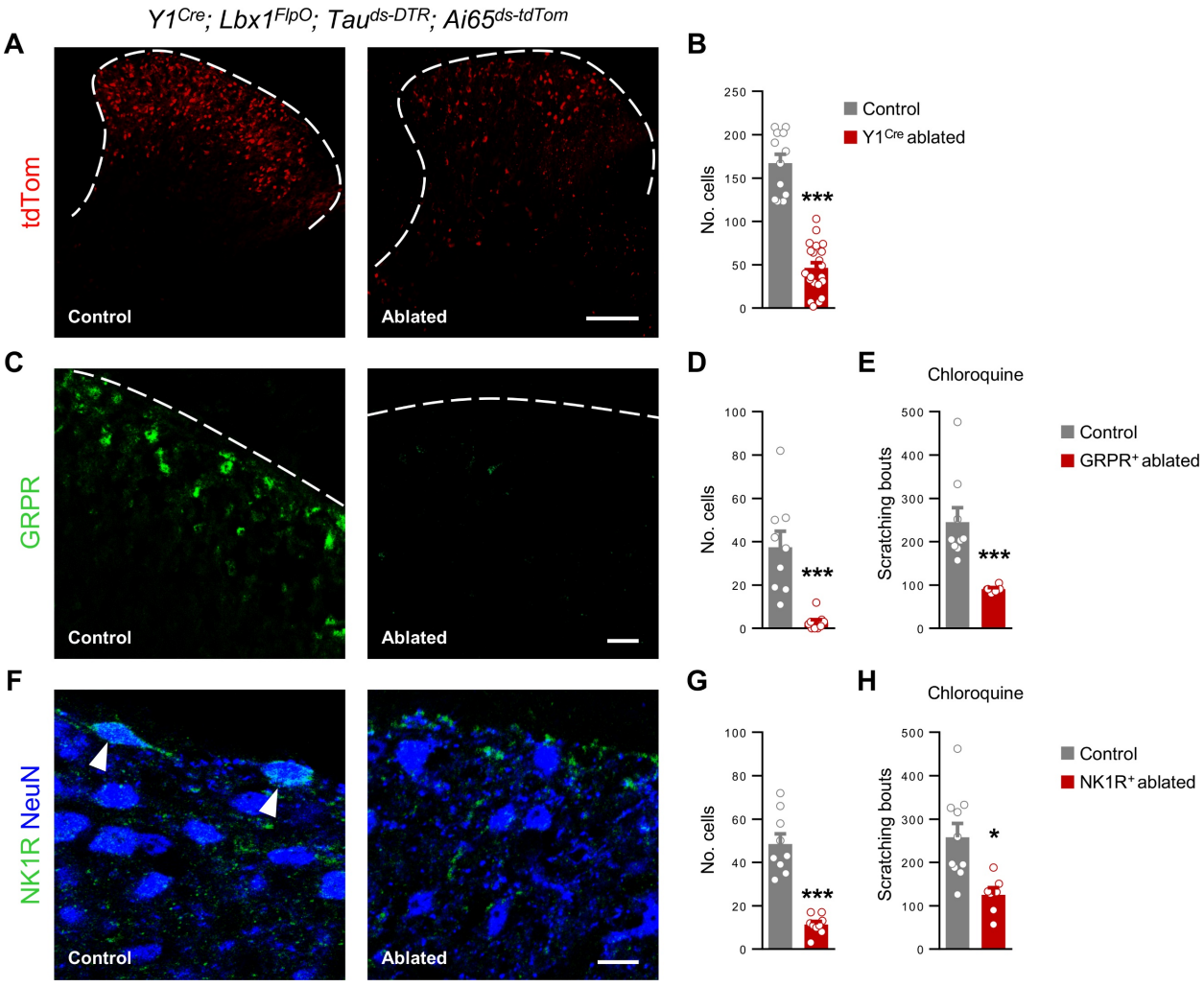

Figure S6 related to Figure 3. Efficiency of cell ablation.

(A) Sections of lumbar spinal cords from P49 *Y1^{Cre}; Lbx1^{FlpO}; Tau$^{ds\text{-}DTR}$; Ai65$^{ds\text{-}tdTom}$* mice treated with saline (control; left) or DT (ablated; right). Scale bar: 100 µm. **(B)** Summary of Y1^{Cre} neuron ablation efficiency (control, 6 cords; ablated, 7 cords; 3 sections per cord). (**C)** Sections from P42 wild type mice showing loss of GRPR immunoreactivity in the superficial dorsal horn at the cervical level 2 weeks after treatment with control SAP (left panel) or BOM-SAP (right panel) to ablate GRPR^{+} neurons. Scale bar: 20 µm. **(D)** Summary of GRPR^{+} neuron ablation efficiency (control, *n* = 3 mice; ablated, *n* = 3; 3 sections per cord). **(E)** Chloroquine-induced scratching is reduced in wild type mice 2 weeks following treatment with BOM-SAP (*n* = 6; controls, *n* = 8). **(F)** Sections from P42 wild type mice showing loss of NK1R immunoreactivity in the superficial dorsal horn at the cervical level 2

weeks after treatment with control SAP (left panel) or with SSP-SAP (right panel) to ablate $NK1R^+$ neurons. Scale bar: 10 µm. **(G)** Summary of $NK1R^+$ neuron ablation efficiency (control, $n = 3$ mice; ablated, $n = 3$; 3 sections per cord). **(H)** Chloroquine-induced scratching is reduced in wild type mice 2 weeks following treatment with SSP-SAP ($n = 7$; controls, $n = 10$). *$p < 0.05$, ***$p < 0.001$. Data: mean ± SEM.

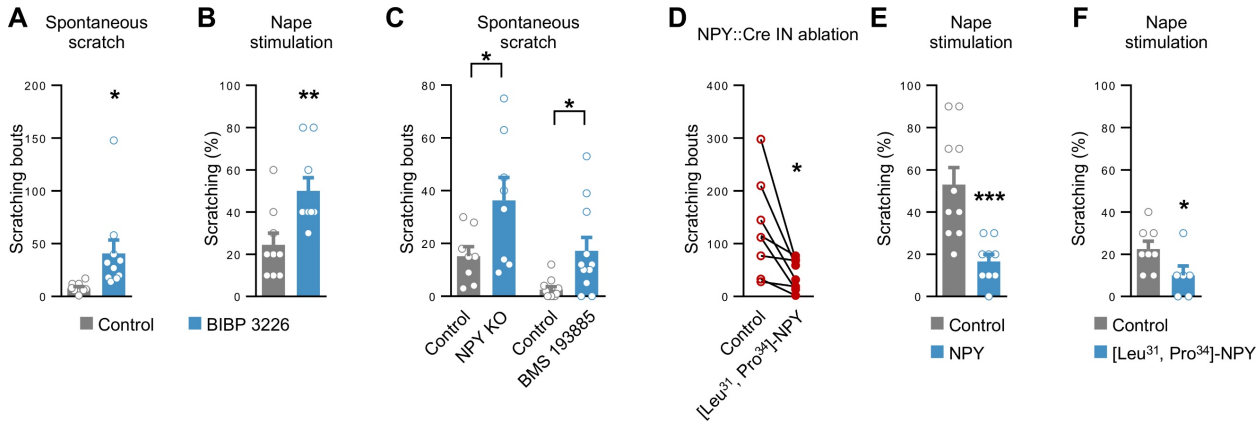

Figure S7 related to Figures 6 and 7. Y1 receptors modulate mechanical itch.

(A and B) I.t. injection of BIBP 3226 (5 µg in 10 µl) increases both spontaneous (A; $n = 10$; controls, $n = 10$) and evoked (B; $n = 9$; controls, $n = 9$) scratching. **(C)** Disruption of NPY-Y1 signaling increases spontaneous scratching in global NPY KO mice ($n = 8$; littermate control, $n = 8$), or following i.p. injection of wild type mice with the Y1 antagonist BMS 193885 (1 mg kg^{-1}, $n = 11$; vehicle, $n = 11$). **(D)** Spontaneous scratching in *NPY::Cre; Lbx1^{FlpO}; Tau$^{ds\text{-}DTR}$; Ai65$^{ds\text{-}tdTom}$* mice 1 week after DT treatment is reduced by i.t. injection of the selective Y1 agonist [Leu^{31}, Pro^{34}]-NPY (1.5 ng in 10 µl; $n = 8$) compared with vehicle. A two-tailed, paired t-test was used to assess statistical difference. **(E)** Evoked scratching is reduced when mice are injected with NPY (100 µg kg^{-1}, i.p., $n = 9$; vehicle, $n = 10$). **(F)** Scratching in response to nape stimulation is reduced following i.t. injection of [Leu^{31}, Pro^{34}]-NPY ($n = 6$; controls, $n = 8$). *$p < 0.05$, **$p < 0.01$, ***$p < 0.001$. Data: mean ± SEM.